CHALMERS
UNIVERSITY OF TECHNOLOGY

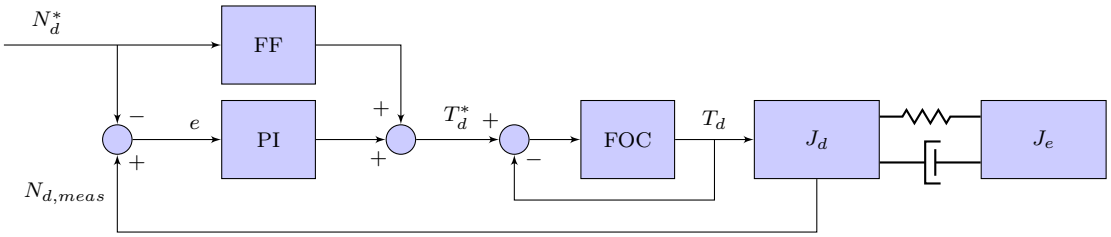

Development of a Method on how to Model a Dynamometer for Driveline Testing

Master's thesis in Systems, Control and Mechatronics

Tobias Glans
Oskar Kärnell

Department of Electrical Engineering
CHALMERS UNIVERSITY OF TECHNOLOGY
Gothenburg, Sweden 2018

Master's thesis EX112/2018

Development of a Method on how to Model a Dynamometer for Driveline Testing

Tobias Glans & Oskar Kärnell

CHALMERS
UNIVERSITY OF TECHNOLOGY

Department of Electrical Engineering
Division of Systems and Control
Mechatronics research group
Chalmers University of Technology
Gothenburg, Sweden 2018

Development of a Method on how to Model a Dynamometer for Driveline Testing
Tobias Glans & Oskar Kärnell

Supervisor: Ingemar Andersson, Volvo Cars
Examiner: Jonas Sjöberg, Electrical Engineering

Master's Thesis EX112/2018
Department of Electrical Engineering
Division of Signals and Systems
Chalmers University of Technology
SE-412 96 Gothenburg
Telephone +46 31 772 1000

Typeset in LaTeX
Gothenburg, Sweden 2018

Development of a Method on how to Model a Dynamometer for Driveline Testing
Tobias Glans
Oskar Kärnell
Department of Electrical Engineering
Chalmers University of Technology

Abstract

During development of engines a device that can apply braking torque is used to simulate the load that the engine would experience in a vehicle. This device is called dynamometer and is connected to the engine via a shaft where it can control the load the engine is subject to. Modern testing is becoming more advanced, demanding more precise resemblance of vehicle load from the dynamometer. This defines a need for knowledge about the dynamometer control performance.

This thesis describes a method for modelling a dynamometer including control system and shaft, using system identification. The system can essentially be divided into three main parts: speed controller, torque control including electrical part of the dynamometer and finally the shaft. Experimental data served the identification of the speed controller and shaft. The dynamics of the torque control could not be modelled due to low sample rate in the experiment data. Since the torque control is fast and accurate compared to the model of speed controller and shaft this is not a major concern however. The speed controller could be modelled quite accurately. Additional experiments is however needed to analyse and verify some features of the speed controller. The reason is that the speed controller seemed to consist of a feedback- and a feedforward term and the feedforward term can only be found by excitation of the speed demand value, which was limited in the experiments performed. The shaft was estimated as a mechanical two mass model which seems to explain the most prominent dynamics of the shaft, based on experiment data. Among the different models, the shaft model has the most potential for refinement. To enable this, new experiment data with less excitation from the engine is needed however. This is because the engine torque is not measured but exists as an input. This requires the engine torque to be considered noise during the system identification procedure.

Keywords: Dynamometer, Engine, System Identification, Driveline Test System, Torque Control, Speed Control.

Acknowledgements

We would especially like to thank Ingemar Andersson Technical Expert – Correlation and Measurement Technology at Volvo Cars Torslanda and Jonas Sjöberg Professor - Mechatronics at Chalmers univerity of technology for sharing their deep knowledge and guiding us through the project.

We would also like to thank Ulf Lind Manager - Test Preparation and Methods at Volvo Cars Torslanda for giving us the opportunity to write this thesis.

Finally we would like to thank all the people working in relation to the test cells at Volvo Cars Torslanda that took the time to share their knowledge about the system with us.

Tobias Glans and Oskar Kärnell, Gothenburg, December 2018

List of Symbols

J_d	[Kgm^2]	Dynamometer inertia
J_e	[Kgm^2]	Combustion engine inertia
K	[Nm/rad]	Spring constant of shaft
B	[Nm/$\frac{rad}{s}$]	Damping ratio of shaft
T_d^*	[Nm]	Electromagnetic torque demand value to frequency inverter
T_d	[Nm]	Electromagnetic torque acting on the asynchronous machine
$T_{d,shaft}$	[Nm]	Torque acting on the shaft by the asynchronous machine
T_e^*	[Nm]	Torque demand value for the combustion engine
T_e	[Nm]	Torque developed by the combustion engine
T_{ff}^*	[Nm]	Torque demand value, feedforwrd term
α_e^*	[%]	Throttle demand value for the combustion engine
α_e	[%]	Throttle for the combustion engine
N_d^*	[rpm]	Dynamometer speed demand value
N_d	[rpm]	Dynamometer speed
N_e^*	[rpm]	Combustion engine speed demand value
N_e	[rpm]	Combustion engine speed
$N_{d,meas}$	[rpm]	Dynamometer speed measurement
$N_{e,meas}$	[rpm]	Combustion engine speed measurement
$T_{d,meas}$	[Nm]	Dynamometer torque measurement
$T_{d,calc}$	[Nm]	Fast electromagnetic torque estimation
$T_{d,shaft,calc}$	[Nm]	Estimated shaft torque calculated from $T_{d,calc}$ and a motion model of the system
f_{cb}	[Hz]	Frequency of the combustions created by the engine

List of Abbreviations

ARMAX autoregressive moving average exogenous input. 8, 13, 30, 59
ARX autoregressive exogenous input. 7–10, 13, 52, 54–56

BS binary sequence. 33, 34, 45

CAE computer aided engineering. 1

DTB dynamic test bed. 15, 17–20, 22–24, 35, 43, 75

ECM engine control module. 15
EMS emission measurement system. 16

FF feedforward. 42–44
FIR finite impulse response. 38
FOC field oriented control. 6, 23, 27–29, 35, 42–44, 52–55, 57, 68, 75

HIL hardware in the loop. 15

MIMO multiple input multiple output. 43, 58, 59

OE output error. 8, 52, 55, 56

PI proportional-integral. 42–45, 49, 63
PWM pulse width modulation. 17

SC speed control. 23, 26, 27, 29, 32, 45, 57, 63, 66–68, 75
SISO single input single output. 13, 43, 44, 57, 58
SITB system identification toolbox. 8, 12, 45, 59
SNR signal to noise ratio. 45, 64

TB test bed. 15, 18, 19, 22, 23

UUT unit under test. 15, 16

Contents

1
Introduction

1.1 Background

During development of engines and drivelines, extensive testing is performed to validate functionality and performance. A widely used tool in this process is the dynamometer, an electric induction machine that is connected to the test object via a drive shaft. The purpose of the dynamometer is to apply a torque that resembles that which the driveline would experience in a driving car. This way measurements can be performed in a lab for evaluation of the engine and driveline performance before the vehicle is tested on the road. The whole setup is controlled by an automation system that controls the dynamometer and the engine by sending speed or torque demand values.

Up to now, tests using the dynamometers studied in this thesis has mainly been performed under relatively constant conditions. In modern testing a need for more fast dynamic control is coming up. There exists equipment that can handle this and can for example simulate wheel slip (a sudden loss of torque on the wheel, caused by for example ice on the road). In general a test cell is very expensive however and one want to make use of already installed cells as much as possible. This defines a need of evaluating what the system at hand is capable of. There might be properties of the dynamics that limits which test scenarios that can be performed. This could mean that it is not possible to actuate too fast changes in torque set points.

One might want to evaluate how the driveline reacts to rapid changes in either torque or speed on the axle. However there is no use trying to run such a test if the dynamometer system (see Figure 3.1) isn't able to realise the torque or speed needed. It is important to know if this is the case or not beforehand to not waste resources running insufficient tests. To be able to do this one needs a dynamic model of the dynamometer system, i.e. a description of it. Using this model one can simulate how well complex demand values in torque or speed can be followed. It follows that based on that one can decide if the dynamometer system at hand is suitable for the test one wishes to perform. Such a simulation model could also be of use in computer aided engineering (CAE) at the engine side. They could use it to deduce if wear on engine parts may be due to phenomenon caused by the dynamometer control that would not occur in a real vehicle on the road. One more thing of interest is to what extent and at which speed the shaft connecting the dynamometer and the engine introduces resonant behaviour in the system. Knowledge about this

can be useful when designing tests to perform in a test cell.

1.2 Contributions

The main contribution of this thesis is the development of a method on how to obtain a mathematical model of the dynamometer including control system and shaft at Volvo Cars Torslanda. This has been done by performing all steps in that process ranging from gathering information about the system up to model validation. To begin with the dynamometer setup has been surveyed, which is described in Chapter 3. There the system setup is described together with possible control modes and available signals. System and signal properties that may affect the results of system identification are highlighted.

Experiments aiming to provide data for successful system identification has been designed and executed in test cell. Based on the data obtained and results from system identification a revision on the experiments has been made. Here the most useful tests are pointed out and additional new tests are proposed.

System identification has been used to derive a simple simulation model of the dynamometer including control system and shaft. The complexity of the model is limited by the data that was obtained during experiments. It can describe the most important dynamics in the system however and serves as a good starting point in modelling the system. Difficulties encountered and assumptions made in the modelling has been commented on and is something that has to be taken into account in future work.

1.3 Delimitations

This section defines delimitations in this project. They provide a quick overview on possible improvements to consider in future work.

- Experiments are performed on existing hardware without any modifications.
- Experiments are performed with the dynamometer connected to a gasoline engine only.
- No advanced model of the combustion engine is used in simulations. It is assumed to have known inertia and stiff mechanics.
- The electromagnetic torque calculated by the system is assumed to be correct.
- The shaft is not analysed in its various parts but rather as a single unit.
- Experiments are not designed to excite both sides of the system at the same time.
- Experiments designed to excite the system by changing the speed reference in dynamometer speed control mode are limited to slow ramps.

1.4 Thesis Outline

This thesis contains 8 chapters. The first chapter gives an introduction on what the thesis is about. The second chapter gives theory relevant for the chapters to follow. Chapter 3 contains a description of the system that is the test cell that has been used in this project. This is followed up by Chapter 4 that is about experiment design aiming to provide data for system identification of dynamometer including control system and shaft. In Chapter 5 analysis of the data obtained through experiments is performed. Chapter 6 contains modelling and system identification of the dynamometer including control system and shaft. Here the model that was obtained is derived and discussed about. Chapter 7 includes some analysis used to validate the claims made about the model in previous chapter. The thesis is concluded in Chapter 8.

2
Theory

This chapter introduces the most relevant theory used in this thesis.

2.1 Periodicity of Combustion Engine

The purpose of the dynamometer setup studied in this project is to allow for the testing of combustion engines that are in development at Volvo Cars. A basic understanding of how a combustion engine works is necessary when designing tests for the dynamometer setup that requires the combustion engine to be connected to the dynamometer. It is important to know that when running the dynamometer with the engine connected, both the combustion engine and the dynamometer might excite the system based on the mode the system is set to run at. When the dynamometer is set to speed control it compensates for the excitation that the combustion engine delivers to the system, with the specific condition that the combustion engine always to some extent are exiting the system. This excitation come from the combustions that the engine creates, which in this case is two with each rotation, because the object used for testing is a four cylinder four stroke engine. The frequency the combustion engine creates based on the speed of rotation can easily be calculated as

$$f_{cb} = 2N_e/60, \tag{2.1}$$

where f_{cb} are the frequency of the combustions in Hertz and N_e is the current speed of the combustion engine in rpm. It is also uncommon for each cylinder in a combustion engine to perform identically, this can result in a rhythmic pattern for each rotation, i.e two combustions, $f_{cb}/2$ and might also be seen in cycles i.e four combustions $f_{cb}/4$.

2.2 Induction Machine and Field Oriented Control

An induction machine is typically a three phase electric motor or generator. Its main parts are the housing that is the stator and the rotating part named rotor. The rotor is placed inside the stator with a small distance in between called air gap. The three phases are winded geometrically in the stator so that the alternating current produces a rotating magnetic field. An interaction between this rotating field and currents induced by the stator windings into the rotor produces torque. For currents to be induced in the rotor there has to be a relative speed between the

rotating magnetic field and the mechanical rotation of the rotor [1]. This relative speed is called slip speed and affects how much torque is produced.

Field oriented control FOC is a common way to control induction machines when the objective is to follow a specific speed or torque demand value. In FOC the fact that the stator currents can be divided into two orthogonal components i_q and i_d is used. i_q corresponds to torque producing current and i_d corresponds to magnetic flux producing current. i_q and i_d is related to the three phase currents in the stator by a matrix transformation called $dq0 \rightarrow abc$ transformation. The torque can thus be controlled independently by the magnitude of i_q. This is done by transforming the reference values of i_q and i_d to the three phase references for a frequency inverter controlling the induction machine [2].

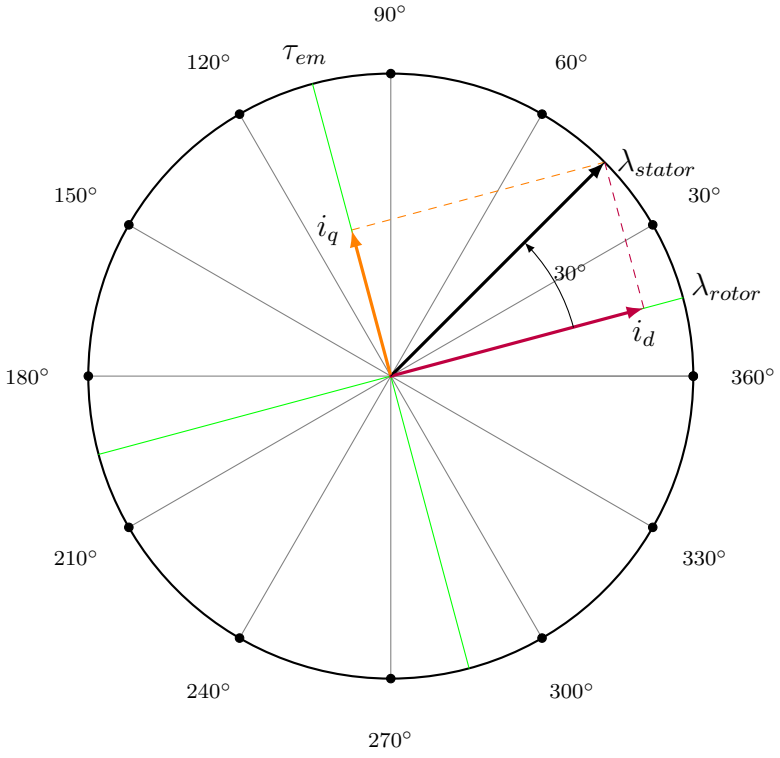

Figure 2.1: From this figure it is possible to see that the direct current i_d is placed in the same direction as the rotor flux vector λ_{rotor}. Because i_d is actively placed in the direction of λ_{rotor} it will produce a magnetic field component for λ_{stator} that only affects the flux in the rotor and hence does not produce torque. The same is true for the quadrature current i_q that is placed 90° out of sync and will therefore produce a magnetic field that directly affects the developed torque produced by the electric machine. Because i_d and i_q are decoupled it is possible to keep i_d constant while changing i_q for the purpose of changing the torque produced by the electric machine. For this to work it is necessary to repeatedly calculate the placement of λ_{rotor}, because this gives the angles for i_d and i_q which the system will produce. Notice that the 30° in the figure is an example and depends on the direct and quadrature currents.

2.3 System Identification

There are two sides of the coin when it comes to modelling dynamical systems. One is that one wants to have model that given an input can predict the system output. Such models are necessarily parameterised (i.e. have parameters defining input output relationship) and are useful especially in simulations. The other important part of system modelling is that one wants to describe qualitative properties. This includes transient analysis and frequency analysis. Sometimes this is useful for its own sake but it is also a good starting point in the modelling of parameterised models. Approaches to both types of modelling are described in what follows.

2.3.1 Transient Analysis

Transient analysis is performed by analysing the system response to a sudden change in the excitation of the system. Analysing the transients of a step response is the typical example. Transient analysis can typically give information on causal relations between system variables, dominating time constants, delays and static gain. Transient analysis is the most common identification method used in the industry [3] and can give relatively much information based on quite simple experiments. The simplicity is important because care must be taken not to damage the equipment. This is crucial since the equipment and not least downtime, in production is typically incredibly expensive. The fact that step responses are simple to perform does not guarantee that it is safe to perform however. This is discussed further in Section 3.3.

2.3.2 Parameterised Modelling Methods

Transfer function, state space, autoregressive exogenous input (ARX) are all examples of models that uses parameters to describe a system model and is therefore called parameterised modells. These methods come in two more groups named black box modelling and grey box modelling, where grey box modelling uses knowledge of the physical system to choose the model structure and thereafter data to estimate the parameters of this structure.

2.3.3 Linear Black Box Models

A common way to model a system is by defining

$$y(t) = G(q)u(t) + H(q)e(t) \tag{2.2}$$

where y(t) is the output, u(t) is the input and e(t) is a stochastic process commonly assumed to be white noise [4]. By letting G(q) and H(q) be polynomials in q with finite number of coefficients such a model attempts to explain an output sequence in terms of past input and noise sequences. There are several standard ways to define G(q) and H(q) based on knowledge of a system. A common one is the ARX model where $G(q) = \frac{B(q)}{A(q)}$ and $H(q) = \frac{1}{A(q)}$, graphically represented in Figure 2.2. An important benefit using this model is that its predictor defines a linear regression that

enables simple and powerful estimation of the model parameters [4]. A disadvantage is that the coefficients of A(q) must describe the noise properties which may demand high model order to be estimated. This is often handled by suggesting an ARMAX model instead that uses a moving average of the noise in the numerator of H(q) so that $H(q) = \frac{C(q)}{A(q)}$ [3]. If one would suspect that the noise present is mainly pure measurement noise a good model would be the output error (OE) where $H(q) = 1$.

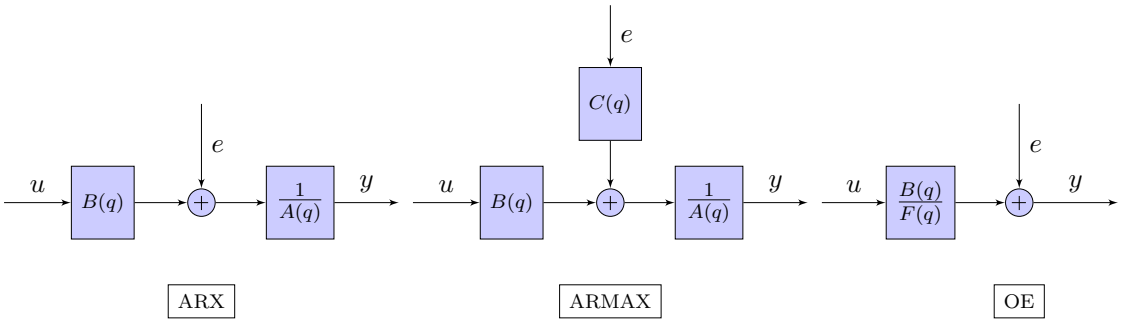

Figure 2.2: A graphical representation of three black box model structures, from left to right are ARX, ARMAX and OE. The noise passes through the system poles in both ARX and ARMAX whereas in OE the noise is added directly to the output and hence hasn't propagated though the system. The ARMAX model structure also lets the noise pass through $C(q)$ which colours the noise before it is propagated through the system. The ARX model on the other hand assumes that the process noise is white. The choice of model structure hence depends on where and how the noise enters the system.

2.3.4 System Identification Toolbox

The system identification toolbox (SITB) (available for Matlab) is the software of choice for parameter estimation of black box models. It provides multiple model structures and various choices of regression algorithms. The toolbox provides a number of plots for studying models and their input, output data. The tools provided by SITB can speed up the system identification process and it has been used extensively in this project.

2.3.5 Residual Analysis

To get insight into the quality of a dynamic model G one can study the cross-correlation between the input u and the residuals $(y - \hat{y} = y - (Gu + He))$. A good dynamic model doesn't have significant correlation between the input and the residuals (cross-correlation). To get insight into the quality of the noise model H (if there is one) one studies the autocorrelation of the residuals (the correlation with oneself). A good noise model H colours the noise e in the same way as the real system, resulting in an insignificant autocorrelation of residuals which are indicated by the use of confidence regions. Figure 2.3 and Figure 2.4 gives an example of some information that can be extracted from residual plots.

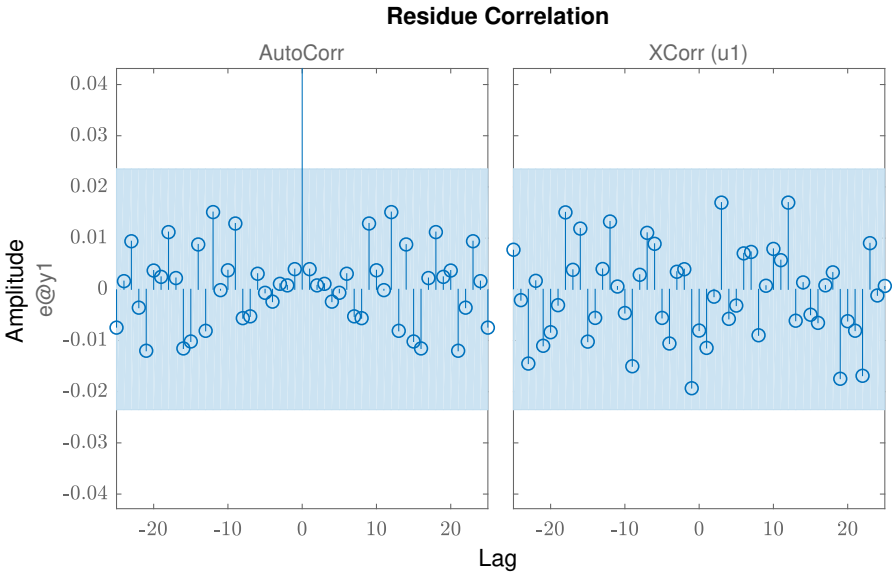

Figure 2.3: This figure shows the residuals of an ARX model on data generated by an ARX- model of the same model structure. One can see by looking at the cross-correlation that the input doesn't have any significant correlation between the input and the error and the dynamic model has been able to use the important information in the input to predict the output. Looking at the autocorrelation plot one can see that there isn't any significant correlation within the error which means that the noise model has been successful at whitening the process noise that was introduced to the system. Notice the correlation procedure requires a fixed point to compare to other points which means that the autocorrelation at sample 0 in the plot means a correlation between two of the exact same sample, which of course always are correlated and the fact that it is outside the confidence region of 99% can therefore be disregarded.

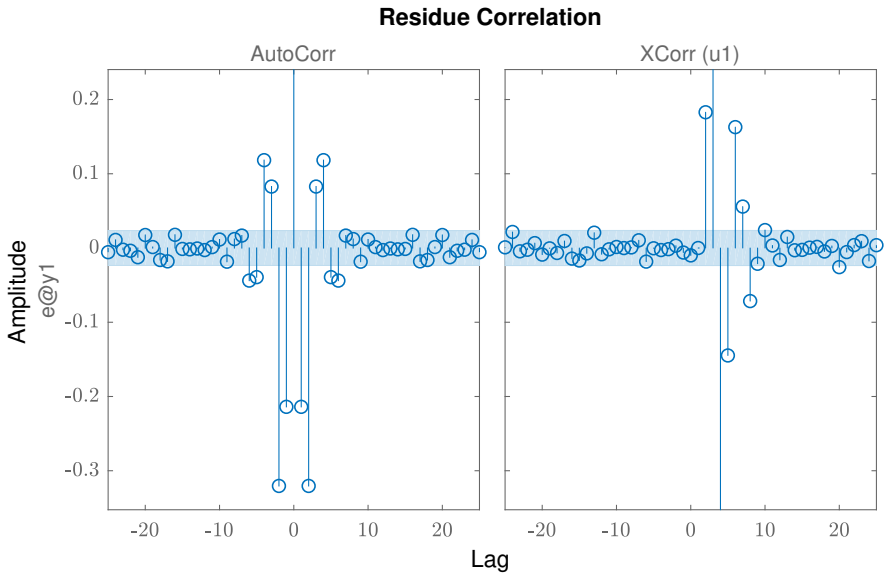

Figure 2.4: This figure is showing the residuals of an ARX model structure when trying to estimate on data generated by a higher order ARX- model. Looking at the cross-correlation it is possible to see that it leaves the confidence region at a few points which means that there may exist information in the input that could be used to minimise the error if another dynamic model had been chosen. Looking at the autocorrelation plot it is possible to see that samples close to the centre are outside the confidence region which gives a hint that there might be high frequency noise in the output that the noise model hasn't been able to explain.

2.3.6 Confidence Regions

Estimated parameters are always subject to uncertainties. The reason is twofold, first because of disturbances in the observed data and second due to possible imperfection in choice of model structure [5]. If we suppose however that the model structure is suitable to describe the true system, then the disturbances are the cause of uncertainty. Large uncertainties in the model parameters means that the model is less trustworthy since the estimated parameters may vary significantly between repeated identical experiments. Since this is an important aspect of the model quality one wish to evaluate how much the parameter estimates may vary. This is done by forming confidence intervals for the parameter estimates.

Now suppose that the disturbances are Gaussian so that the residuals becomes Gaussian. Then a confidence interval that with a specific probability contains the unknown true parameter can be formed [6]. The confidence interval is a range of values centred around the parameter mean. When the confidence interval is calculated from a sampled distribution it is given as

$$[\hat{\theta} - t^* SE,\ \hat{\theta} + t^* SE] \tag{2.3}$$

where SE is the standard error and t^* is derived from the 97.5 % quantile of the student's t distribution (for a 95 % confidence interval). For large number of samples this approaches the standard normal distribution which can then be used instead [7].

The above mentioned confidence interval calculation is valid for the uncertainty of specific parameter estimates. Sometimes it is of greater interest to know a combination of estimated parameters. A typical example is the pole-zero placements of a linear dynamical system. These affects dynamical properties such as response time and stability and their placement is dependent on a combination of n number of parameter values i.e it is a multivariate function of the estimated parameter vector $\hat{\theta} \in \mathbb{R}^n$. The pole-zero placement is a vector $\hat{\theta}_{pz} \in \mathbb{R}^2$ obtained through transformation of $\hat{\theta} \in \mathbb{R}^n$. The confidence region of $\hat{\theta}_{pz}$ takes the form of an ellipse and is dependent upon the covariance matrix C_{pz} of $\hat{\theta}_{pz}$. Under the assumption that $\hat{\theta}$ is Gaussian with small variance it is possible to apply the Delta Method to approximate C_{pz} as

$$C_{pz} = J(\hat{\theta}_{pz}) C J(\hat{\theta}_{pz})^T \tag{2.4}$$

where $J(\hat{\theta}_{pz})$ is the Jacobian matrix of $\hat{\theta}_{pz}$ [8]. C is the covariance matrix of the estimated parameter vector $\hat{\theta} \in \mathbb{R}^n$. Knowing the covariance matrix C_{pz} enables to calculate the Mahalanobis distance [9]

$$d(\hat{\theta}_{pz}) = \sqrt{(\hat{\theta}_{pz} - \theta_0)^T C_{pz}^{-1} (\hat{\theta}_{pz} - \theta_0)} \tag{2.5}$$

which defines how far off in terms of standard deviations a point is from the distribution mean θ_0. By squaring 2.5 one obtains

$$d^2(\hat{\theta}_{pz}) = (\hat{\theta}_{pz} - \theta_0)^T C_{pz}^{-1} (\hat{\theta}_{pz} - \theta_0) \in \chi^2(2). \tag{2.6}$$

Now $d^2(\hat{\theta_{pz}})$ can be obtained by passing desired confidence level into the inverse Chi-square cumulative distribution function. Now combining the mean $\hat{\theta}_{pz}$, covariance matrix C_{pz} and the Mahalanobis distance one defines the confidence ellipse. [4] The ellipse has its center at $\hat{\theta}_{pz}$ and the semi axes is defined along $d\sqrt{\lambda_i}V_i$ where λ_i and V_i is the ith eigenvalue and eigenvector of the covariance matrix C_{pz} [10]. So in summary this is a way of estimating confidence regions provided parameter estimates $\hat{\theta}$ and covariance matrix C. SITB also implements functionality to plot confidence regions that might use a different method of approximation. These are not easily accessible in the command line and thus the above method provides an alternative.

2.4 Mechanical Two-Mass System

A mechanical two-mass system consist of two masses which are connected with a flexible drive shaft. The main purpose of a drive shaft is to transfer torque between two rotating bodies, where one usually drive the system, for example a motor, while the other acts as a load as shown in Figure 2.5.

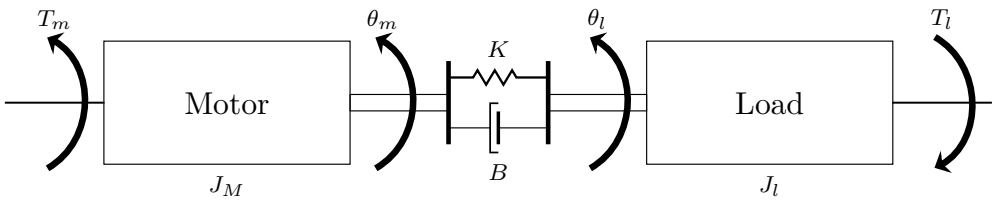

Figure 2.5: An representation of a mechanical two-mass system including a motor and a load. T_m is the developed torque of the motor and T_l is the load torque disturbance. θ_m and θ_l are the angles of the two components

To allow for some misalignment it is common to add universal joints or constant velocity joints at both ends of the drive shaft which helps increase the life span of the drive shaft but has the possibility to add backlash to the system. The torque acting on a flexible drive shaft is dependent on the material properties of the drive shaft and can be modelled as

$$T_s = K(\theta_m - \theta_l) + B(\omega_m - \omega_l), \tag{2.7}$$

where K is the spring constant and B is the dampening constant as described in [11]. In this structure the assumptions are made that the twisting torque is proportional to the difference in angle and the dampening torque is proportional to the difference in rotational velocity. Both K, the shafts ability to flex and B, the shaft internal dampening are dependent on the dimensions and material properties of the drive shaft. The two-mass model also assumes that the shaft inertia is zero, which results in that the shaft inertia J_s is absorbed into the motor J_m and load J_l inertia when identified as a two-mass oscillator. The two-mass system can then be described by

the following equations,

$$\begin{aligned} J_m\dot{\omega}_m &= T_m - T_s = T_m - K(\theta_m - \theta_l) - B(\omega_m - \omega_l), \\ J_l\dot{\omega}_l &= T_s - T_l = K(\theta_m - \theta_l) + B(\omega_m - \omega_l) - T_l, \\ \dot{\theta}_s &= \omega_m - \omega_l, \end{aligned} \tag{2.8}$$

where $\theta_s = \theta_m - \theta_l$ is the shaft-torsion. This can be represented with the following state space form

$$\begin{aligned} \begin{bmatrix} \dot{\omega}_m \\ \dot{\omega}_l \\ \dot{\theta}_s \end{bmatrix} &= \underbrace{\begin{bmatrix} \frac{-B}{J_m} & \frac{B}{J_m} & \frac{-K}{J_m} \\ \frac{B}{J_l} & \frac{-B}{J_l} & \frac{K}{J_l} \\ 1 & -1 & 0 \end{bmatrix}}_{A} \begin{bmatrix} \omega_m \\ \omega_l \\ \theta_s \end{bmatrix} + \underbrace{\begin{bmatrix} \frac{1}{J_m} & 0 \\ 0 & -\frac{1}{J_l} \\ 0 & 0 \end{bmatrix}}_{B} \begin{bmatrix} T_m \\ T_l \end{bmatrix} \\ y &= \underbrace{\begin{bmatrix} 1 & 0 & 0 \end{bmatrix}}_{C} \begin{bmatrix} \omega_m \\ \omega_l \\ \theta_s \end{bmatrix} \end{aligned} \tag{2.9}$$

This model structure represent non active loads such as rolling mills or paper machines. Because the load in these systems aren't active they can be parameterised as a grey box model and identified using a single input single output (SISO) black box structure such as ARX with T_m as input and ω_m as output, hence the chosen C matrix. The number of parameters in the ARX model is chosen as to describe the transfer function from T_m to ω_m in the dynamic model and the transfer function from T_l to ω_m in the noise model as described in [12]. After the ARX has identified the system transfer function one can solve for the grey box parameters using the system equations as shown above together with the ARX identified model. The parameter identification as described in [12] has been successful at estimating the model parameters when measuring T_m and ω_m for loads with the same or larger inertia than the motor itself. When the inertia of the load is to small it does not bend the shaft enough to allow for successful parameter estimation and the system does look like a one-mass system. Adding a T_s sensor helped with this problem because the oscillations that wasn't easily seen in ω_m was much more apparent in T_s.

Parameter estimation on an active load such as a combustion engine is more difficult. In [13] they use knowledge of the nonlinear friction in the cylinders of the combustion engine to create a state space structure that they want to identify. In this case they use a high order ARMAX structure because the noise isn't white when it is introduced to the system. In this study they use an unfired engine, which means that the engine isn't on during the experiment. This is because they do not want the excitation to be to large in comparison to the excitation from the driveline it is connected to.

Both of these papers has in common that they want to get the parameter values to their grey box structure for the purpose of designing a controller. Neither of these reports has any intention of changing components in the system once the identification procedure is complete. In a dynamometer test bench, the load is changed when all tests has been run on that specific load (test object). This could possibly have an affect on the identified system parameters.

3
System

This chapter describes the test cell system that has been worked with in this project. Mainly dynamic test bed (DTB) has been considered but some remarks on test bed (TB) is included. The information in this chapter has been obtained through various discussions with the people working in relation to the test cells together with some system documentation and what has been observed in the data gathered from experiments.

3.1 Dynamometer Setup

A complete dynamometer setup contains many subsystems for controlling the test environment. Some systems exists to take measurements while others are supplying electric power, fuel and other resources to the various parts of the system. The most important parts of the dynamometer test bench are shown in Figure 3.1 and a short summary of their objectives are shown in the list below.

1. Dynamometer setup: Contains the subsystems that are included in the model of the dynamometer and these systems are represented as green in Figure 3.1.
   (a) Control System: Can generate reference signals for the engine and dynamometer to follow and also use the reference from an external source, this is how it is used at Volvo Cars.
   (b) Frequency Inverter: Receives torque reference and delivers current to the dynamometer to make the dynamometer torque follow the reference.
   (c) Dynamometer: Is an asynchronous machine controlled by the frequency inverter. It is directly connected to the combustion engine with a shaft and is controlled by either torque or rotational speed as reference.
2. Engine setup: contains the subsystems that relates to the unit under test (UUT), in other words the combustion engine that is being tested, represented as red in Figure 3.1.
   (a) Engine: The combustion engine is controlled by the engine control module (ECM) and is connected directly to the dynamometer via a shaft.
   (b) ECM: The engine control module is the brain of the motor and decides in what pattern the engine should fire its cylinders and also decides when to burn out waste from the motor. It receives a reference in throttle angle from the control system and decides from that how to run the motor.
   (c) HIL: Stands for hardware in the loop and simulates the signals of the real car. This is a necessary part because the ECM does not allow the motor to start if not the right conditions are met.

3. Support system: contains subsystems that are essential for the testing environment, but doesn't need to be included in the test bench model. These subsystems are represented as blue in Figure 3.1.
   (a) Measured data: The data collected during testing are stored on a server.
   (b) Automation System: The automation system is responsible for controlling many things in the test cell. The temperature of the room is a good example and it is also responsible for sending the reference signals to the control system and saving the measured data.
   (c) EMS: An emission measurement system connected to the the engine. This system gives feed back on the composition of various gases in the gas exhausted by the combustion engine.
   (d) Inca: System that measures various signals and sends them to the automation system.

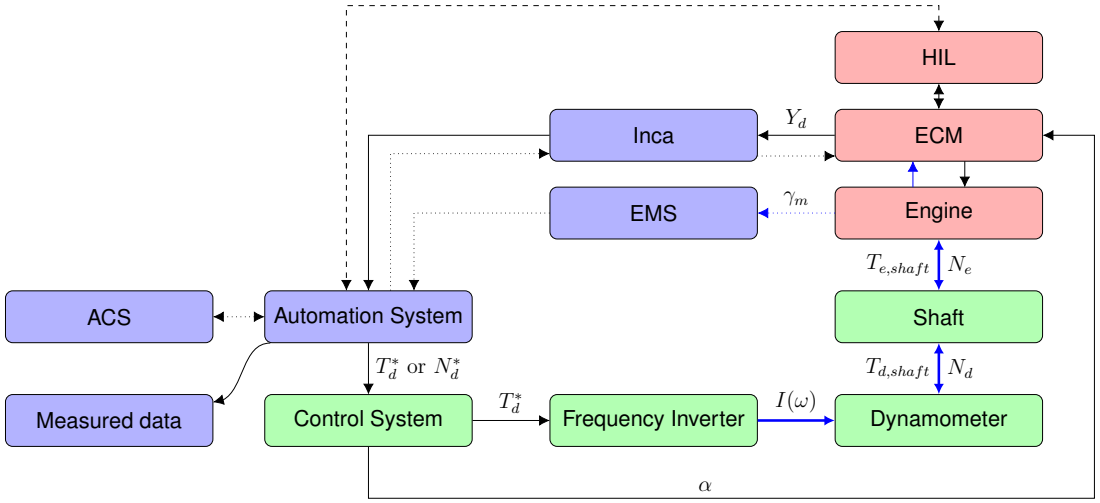

Figure 3.1: Graphical representation of a test bench for driveline testing. The green boxes represent the part of the equipment that is to be modelled in this project. This part is described in more detail in Figure 3.2. The blue boxes are remaining equipment that belongs to the test bench while the red boxes describes the unit under test (UUT) i.e. the combustion engine. Thick blue lines represent physical quantities while thin blue lines represent their measured values. Black lines describes analog and digital signals and dotted lines are functionality beyond interest in this project. Dashed lines represent signals that are used in some cases but not always. α represents the throttle angle of the car, γ_m is exhaust gases passed to the emission measurement system (EMS) and Y_d is data logged from the engine control.

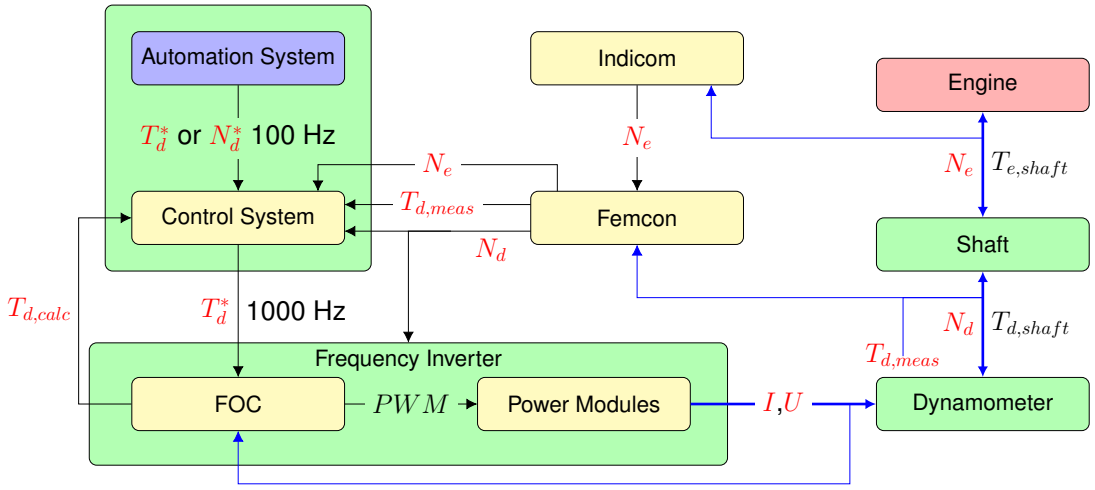

Figure 3.2: Graphical representation of how the system looks like in a DTB test cell. The box named Control System is an interface between the automation system and the frequency inverter. It also has functionality to run the engine and dynamometer manually from the front panel without the automation system. The frequency inverter controls the dynamometer via the three phase voltage U and current I using pulse width modulation (PWM). Available signals are marked in red. T_d^* & N_d^* are reference values for torque and speed on the shaft at the dynamometer side. One of them are passed to the frequency inverter for control and the the other is used for controlling the engine (note that this arrow is excluded from the figure). N_d and N_e corresponds to the speed of the dynamometer and engine respectively while $T_{d,shaft}$ and $T_{e,shaft}$ corresponds to the shaft torque on both sides of the shaft. The standalone yellow boxes are equipment handling measurements.

3.2 Control Modes for the Dynamometer Setup

The dynamometer system currently has several control modes to choose from where only one of them is used in daily operation. The first one is speed control mode which means that the dynamometer controls the speed and the engine controls the torque by changing the throttle. It is also possible to let the engine take throttle reference instead of torque. The second mode (that is rarely used) is the torque control mode, when the dynamometer controls the torque and the engine controls the speed. In this mode the dynamometer is controlling its electromagnetic torque and not the torque that acts on the shaft. The supplier of the system allows the user to purchase extra functionality that unlocks a third mode for their dynamometer systems which is a shaft torque control mode. This control mode is supposed to be used for tests that requires control of the torque that acts on the shaft for example wheel slip simulations. Testing has been done in both the speed control mode and the torque control mode. The shaft torque control mode has not be studied.

3.3 System Limitations

The shaft connecting the engine and the dynamometer together is subject to stress even during normal operation which decreases its lifetime. To minimise wear, violent treatment of the shaft is avoided as much as possible. In normal operation the dyno often controls the speed at a constant level for some time and later changes, at a relatively slow rate, to a different speed. This means that the torque is limited in magnitude and large torque oscillations in the shaft is avoided. However there has been issues with the shaft in the past where the shaft has gotten broken when connected to certain engines. Therefore the personnel in charge of the test beds does not allow for too violent treatment of the shaft during testing. This is an important aspect of the test design in this project since tests designed for system identification could vary quite a lot from normal operation.

The dynamometer system is subject to limitations in the dynamometer (asynchronous machine) and frequency inverter. Some of these limitations exist to protect the dynamometer from being damaged and others from the physical limitations of the system itself. The frequency inverter has a manually set limit in the max and min current to flow through the dynamometer $i_{min,inverter} \leq i_{inverter} \leq i_{max,inverter}$ for the purpose of protecting it. These current saturations are not included in the model of the dynamometer setup and it is therefore important that the data from the system stays within the boundaries of the saturation as to not be affected by it.

3.4 Sensors

The most important sensors for the identification process is the torque and speed sensors. Both a torque and a speed sensor is available on the dynamometer side but only a speed sensor is available on the engine side. The speed sensors are of the same type in both DTB and TB but this is not the case for the torque sensor. In DTB

the stator of the motor is cradled (able to rotate) and an arm with a load cell is connected to it, holding the stator in its place. This allows for torque measurement of the electrical torque, the total torque produced by the motor. In TB this is different and there is instead a torque flange added to the dynamometer side of the shaft and this is used to measure the shaft torque.

3.4.1 Accuracy of the Speed Encoders

The speed encoders are using six leads where two of the leads sends pulses when the sensor rotates and the last four are voltage and ground. A rotary encoder is a discrete sensor and its resolution is therefore bound to the number of slits in the rotating encoding disk. A discrete speed encoder is however able to accurately estimate the speed between each of these slots and they are very resilient to signal noise because it records signal flanks and not any precise measurement of the voltage. The speed encoder is mounted on the stator housing and essentially records the speed difference between the stator and the rotor. This makes the encoder susceptible to vibrations in the housing because it isn't able to differentiate between flanks caused by the rotor and flanks caused by the stator vibrating.

3.4.2 Accuracy of the Torque Sensors

A calculated version of the electromagnetic torque based on current measurements and an adaptive system model exists in DTB. This calculated electromagnetic torque is based on fast current measurements instead of the significantly slower physical load cell. During operation some of the system parameters that affect the torque calculation changes which results in an estimation error. The resistance in the stator and rotor is such a parameter which changes with the temperature of the dynamometer. The adaptive model hence uses the load cell to update the model parameters to minimise the torque error. Even though a calculated version of the electromagnetic torque might be superior for the purpose of system control it isn't obvious that it would be a better choice than the load cell measurements for the purpose of system identification. This is because the signal delay that can be seen in Figure 6.1 could be compensated for. This compensation would be performed using the dynamometer rotor speed (see Figure 6.2 and compare the acceleration with the time when the electromagnetic torque occurs, which should happen simultaneously (see Figure 6.1).

The dynamometer is able to calculate the electromagnetic torque with a frequency of about $4kHz$ because of the high sample rate of the voltage and current. This results in a neglectable time delay when taking into account that the calculated electromagnetic torque that is internally calculated at about $4kHz$, only is available for the user at a frequency of $250Hz$ (in current configuration). The choice of using measured or calculated electromagnetic torque for system identification boils down to that it is easier to get the signals time synced when using the calculated electromagnetic torque signal, note that the delay of the measured electromagnetic torque might not be in complete samples if the sensor used contains a filter. This is not a problem when the measured signal only is used to update the system parameters.

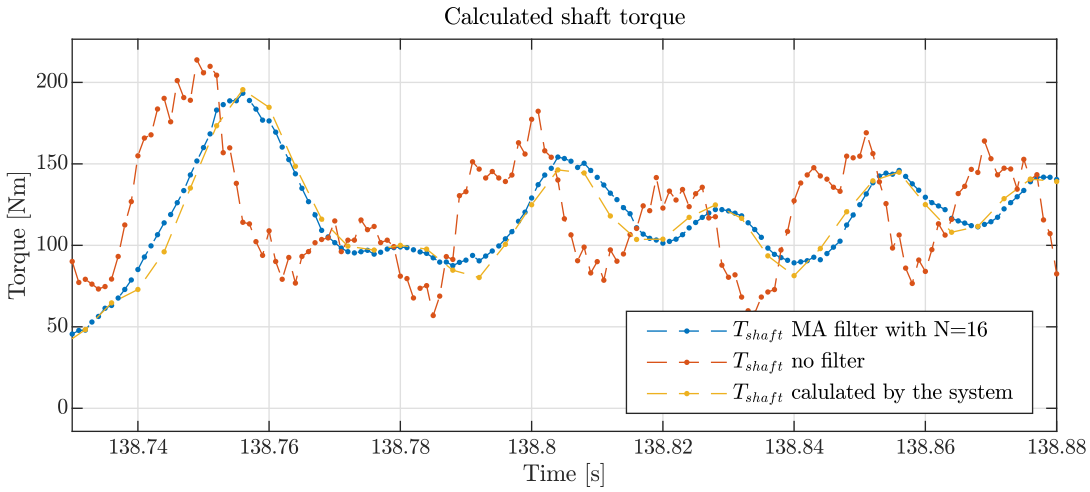

Figure 3.3: A figure showing that filtering N_d using a moving average filter with $N = 16$ before using $\dot{N}_d$ to calculate T_{shaft} gives a result that resembles the calculated version available from the system. The important thing to take from this is that this filtering results in a delay, which either needs to be compensated for or avoided by calculating T_{shaft} using a zero-phase filter instead. The T_{shaft} that is calculated by the system should therefore not be used for identification, instead the calculation should be done manually to avoid the delay.

3.4.3 Shaft Torque Calculation

The system that has been studied in this thesis is called dynamic test bed (DTB) and uses a load cell to measure the electromagnetic torque T_d but no sensor that measures the shaft torque $T_{d,shaft}$. The dynamometer system calculates the shaft torque internally and returns it to the user for analysis. The system is assuming that the friction in the system is zero and can therefore calculate the shaft torque using the Newtons second law for rotation $T_{d,shaft} = J_d\dot{\omega}_d + T_d$. Friction is present in all mechanical systems and the question is to what degree it affects the system. This means that because measurements of both $T_{d,shaft}$ and T_d aren't available, it is not possible to identify the friction with the combustion engine connected. If however the dynamometer would be tested alone it would result in that when $J_d\dot{\omega}_d = 0$ then $J_d\dot{\omega}_d = -T_d - T_{fric} \rightarrow T_{fric} = -T_d$. $\dot{\omega}_d$ is sensitive for speed measurement noise and the system therefore filters ω_d before calculating the derivative. Using a moving average filter with a length of $N = 16$ samples it is possible to get results that looks similar to the shaft torque that the system calculates as shown in Figure 3.3. A symmetric filter of length N results in a delay of $(N-1)/2$ samples. The filtering doesn't seem to differ between various speeds, the speed encoder has 1024 slits which for the dynamometer which is sampled at $1000Hz$ results in 20.48 passed slits every ms at $1200rpm$ and 51.2 passed slits every ms at $3000rpm$. But using the same filter at these various speeds results in the same performance and the same delay on T_{shaft}. Thus the averaging seems to be based on sample rate and not pulses.

3.4.4 Placement of the Speed Encoders

When estimating system parameters for the shaft it is necessary to have shaft torque measurements and speed measurements from the same point on the shaft. The shaft torque, which is defined as shown in Figure 3.5 does not have a corresponding speed measurement from the same point on the shaft. The speed measurements that are available are shown in Figure 3.4 which also shows the optimal placement for the dynamometer and engine speed sensors for the purpose of system identification of the shaft. If sensors were available at these optimal locations it would allow for both T_{shaft} and N_d measurements to be defined at the same point and could then be used as input output signals when estimating the model parameters for the shaft. But because this sensor can't be moved and adding an additional sensor to the system is both time consuming and expensive something else needs to be done to get the speed and torque defined at the same point on the end of the shaft.

The dynamometer squirrel cage rotor is made of aluminium and is able to twist to some extent. However it isn't unreasonable to assume that it is of less significance than the shaft it's connected to. Because measurements aren't available at both ends of the dynamometer its not possible to identify to what extent the dynamometer itself is able to twist and with no other way of getting rid of the dynamometer twist the best choice is to assume that the dynamometer is stiff and let the shaft model absorb the oscillating properties that dynamometer might possess. This affects the estimation of the shaft parameters negatively and might result in different spring and damping parameter values for the shaft. Another look at Figure 3.4 shows that exactly the same problem also occurs for the combustion engine. Even though the combustion engine isn't part of the dynamometer system itself and often replaced, the shaft parameter error is dependent on the combustion engine used during testing but consists of a static model error. The combustion engine is therefore also assumed stiff to make the shaft speed at the optimal position equal the values that are sampled from the actual sensor position.

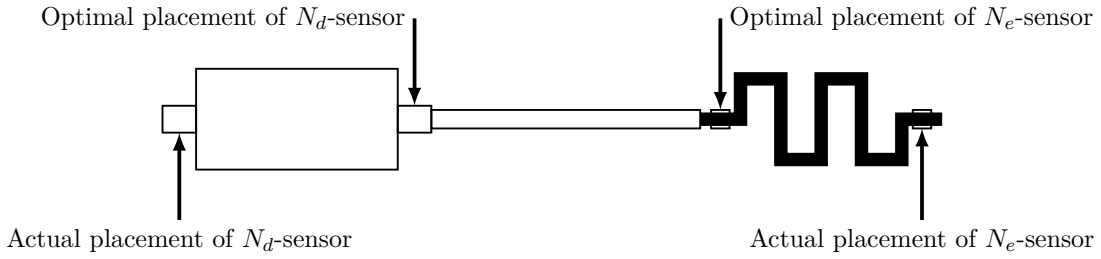

Figure 3.4: The placement of the two speed encoders are shown in this figure. The dynamometer is furthest to the left connected with, through a thin cylinder representing the shaft, the engine which is illustrated as a minimalistic side view of a crankshaft.

3.5 Difference Between DTB and TB

There are two types of test cells, DTB and TB. For the purpose of system identification there are some important differences between these test cells. Test cells of the type TB is using a torque-flange while DTB is using a load-cell which means that TB has measurements of the shaft torque and need to calculate the electrical torque. The same occurs in DTB where the system measure the electrical torque and then calculate the shaft torque. For the purpose of system identification it is important to measure either the shaft torque or the electrical torque. In some cases this isn't possible however. If the dynamometer were to be run without load it wouldn't be able to register any torque measurements from the torque flange. DTB does not have this problem because it is using a load cell and would still provide the measurement of the electrical torque.

Another difference is that in DTB the primary and secondary side of the flywheel are welded together before the combustion engine is put into the test cell. A graphical representation of how the connection between the dynamometer and engine would look like in TB can be seen in Figure 3.5. Another picture showing how the connection would look like in the DTB test cell can be seen in Figure 3.6.

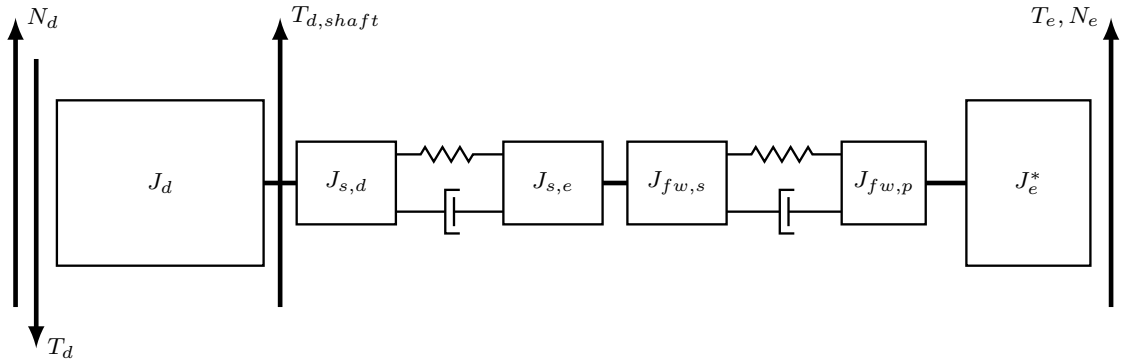

Figure 3.5: A graphical representation of the asynchronous machine, shaft, flywheel and combustion engine as they would behave in a TB test cell, the flywheel isn't welded. $J_{fw,s}$ is the inertia of the flywheel on the secondary side and $J_{fw,p}$ is the primary. $J_{s,d}$ is the shaft inertia on the dynamometer side and $J_{s,e}$ is the shaft inertia on the engine side. These are present to show that shaft inertia exists and possibly isn't homogeneously distributed. In this thesis J_e refers to the total engine inertia in this figure that would be $J_e = J_e^* + J_{fw,p} + J_{fw,s}$.

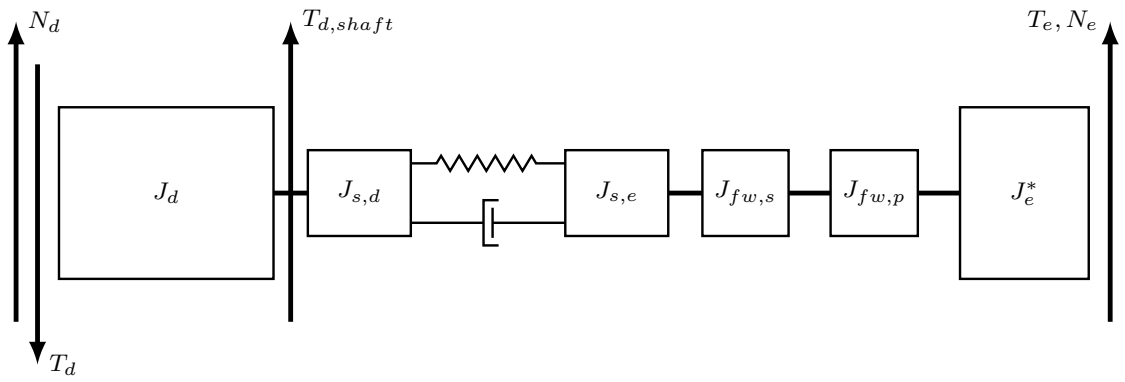

Figure 3.6: A graphical representation of the asynchronous machine, shaft, flywheel and combustion engine as they would behave in a DTB test cell, the flywheels primary and secondary sides are welded together. The parameters in this figure is already described in Figure 3.5

When observing the difference between Figure 3.5 and 3.6 one can see from the first figure (non welded flywheel) behaves as a three mass oscillator and the second figure (welded flywheel) behaves as a two mass oscillator. This observation gives a hint that the order of the models might be different between TB and DTB.

3.6 Dynamics of the Dynamometer Setup

With the system information provided in Chapter 2 and 3 it is now possible to create a system block scheme showing the general signal flow within the system as shown in Figure 3.7. The speed controller (SC) which is only present on the dynamometer side when the dynamometer is set to speed control mode (as described in Section 3.2) is connected in series with the simplified closed loop FOC model. The simplification here is that the FOC will be controlling T_d directly when in reality it is controlling voltages to achieve a current that in turn has a relationship with T_d. The simplification is done because the FOC is a very complex and fast component in comparison to the rest of the system and what is important to model is the ability to follow the reference torque and not the FOC internal anatomy.

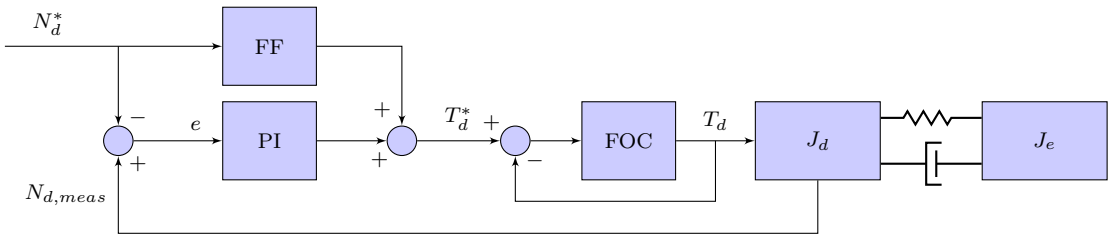

Figure 3.7: A block scheme showing the general signal flow through the system. Notice that the dynamometer speed reference N_d^* enters the feed back part of the system with a negative sign, instead of the much more common positive sign. This is because T_d in this model is defined as the breaking torque and the negative sign has therefore been moved out of the model.

The dynamics of the two mass oscillator can be modelled as shown in Figure 3.6, which show the asynchronous machine, shaft, flywheel and combustion engine as they are connected in DTB. Building on this model with the knowledge from the overall system as shown in Figure 3.2 one can add the two mass oscillator to the other components as shown in Figure 3.7. The signals are defined to be in the same direction as they are in the real dynamometer system at Volvo Cars, this means that T_d is defined as the braking torque on the dynamometer which means that $-T_d$ is the torque that accelerate the dynamometer in the direction of N_d as shown in Figure 3.5 and 3.6.

4
Experiment Design

This chapter introduces all tests that were designed in this project. First the naming convention that has been used for labelling of the different experiments is described. After that the experiments designed are described starting with the tests that resulted in the most useful information of the system. That is then followed up with tests that were either redundant or unsuccessful.

4.1 Naming Convention for Experiments Designed

As already stated in Section 3.2 on page 18 there exist two main modes of operation for the dynamometer system: speed control and torque control. It is possible to excite the system from the dynamometer or the combustion engine in either of these modes and for convenience each test is combined with a label with the following naming convention, **{test name}_{excitation signal}_{control mode}**. The **{test name}** is short description of the test and **{excitation signal}** is either T or N depending on if the excitation is coming from a change in torque or speed reference. The last part of the label **{control mode}** also has two possible states, one for each of the two possible control modes the system can be in. The control modes are differentiated using two letters where the first letter represent the reference signal that the dynamometer is receiving and the second letter the reference signal that the combustion engine is receiving. NT is hence dynamometer speed control mode and TN is dynamometer torque control mode. A test with sinusoidal torque input on the dynamometer would hence have the following name Sine_T_TN.

4.2 Engine Binary Sequence Test

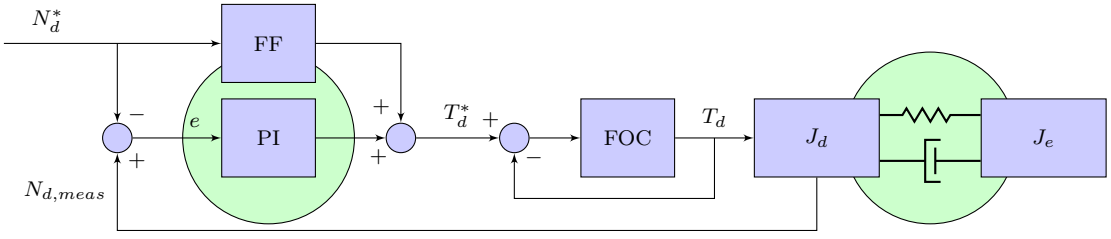

Figure 4.1: Excitation focus of this experiment marked in green.

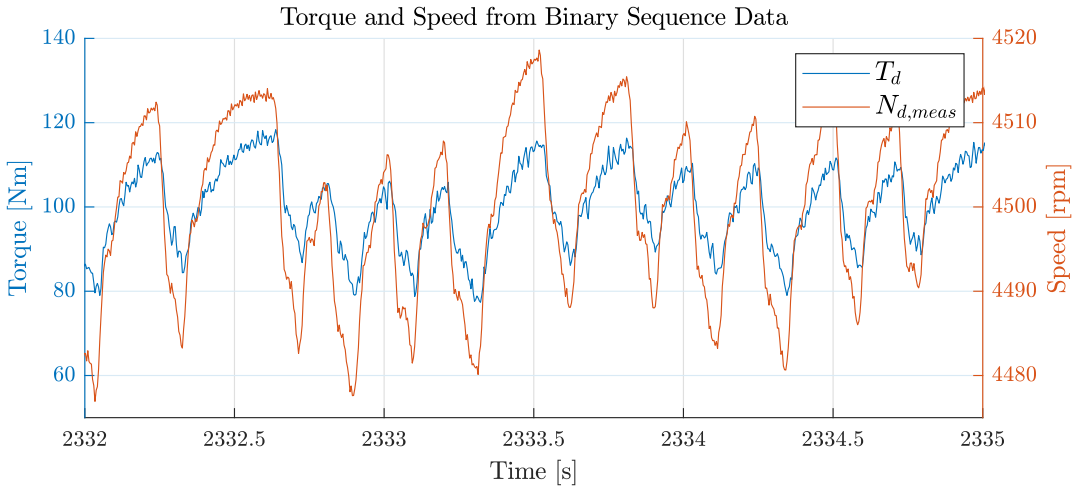

Figure 4.2: Example of binary sequence data obtained from experiment. The data is excited by rapidly letting the engine change the torque produced between two levels.

The idea with this test is to excite the dynamometer system from the combustion engine side by changing at what crank-angle the combustion engine ignites the fuel. By doing this one can change the effectiveness of the combustion and hence the developed torque from one combustion to the next. The test consists of two different crank-angles (ignition-angles) and can switch between these two at the press of a button. By changing the ignition-angle one can achieve two different torque levels resulting in a change of torque that strongly resemble a binary sequence and hence the name of this test. At $1200rpm$ the combustions occur with a frequency of $40Hz$ or every $25ms$ which means that the fastest possible repeated change between two torque levels would be half this, $20Hz$ or $50ms$. The two different crank-angles that were chosen for this test were the optimal combustion crank-angle and a second arbitrary crank-angle chosen for the purpose of resulting in a noticeable torque difference from the optimal crank-angle without resulting in a to rapid increase in temperature which would result in that the test would need to be stopped.

The purpose of this test is to excite the system with a frequency rich input signal when the dynamometer is in speed control mode. The relatively large and rapid changes in torque has an impact on the speed of the dynamometer. This is desired since then the control system is excited in the normal operation mode NT. This test thus overcomes the difficulty to guaranty a low maximum shaft torque when exciting the system with frequency rich changes in the dynamometer speed reference N_NT.

The data obtained from this experiment is particularly useful for estimating parameters of part of the dynamometer speed controller SC. In Section 6.3.1 it was found out that the SC seems to consist of a PI- controller together with a feed forward mechanism. This experiment provides much excitation in when the feed forward is inactive enabling identification of the PI- parameters. It has also been

used in the identification of the shaft. This test was performed by switching manually between the two crank angles. Improvement of this test would be to let software control the change between the different crank angles instead. Doing this one could switch between more than two levels and designing the signal prior to experiment. However this is not recommended to prioritise for now. The main benefit from this test is to estimate PI- parameters and it is sufficient to to this as it is.

4.3 Dynamometer White Noise Torque Test

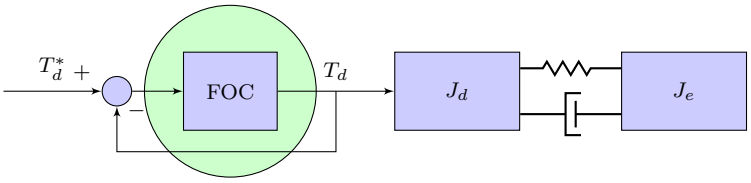

Figure 4.3: Excitation focus of this experiment is marked in green.

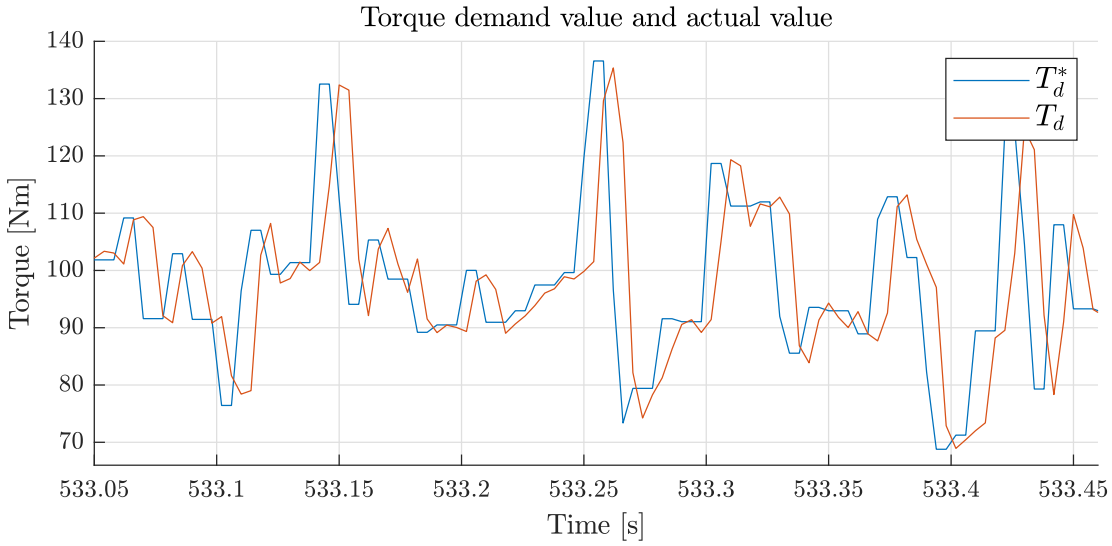

Figure 4.4: Example of white noise torque demand value for FOC. The sample rate of this data is low compared to the dynamics of the FOC.

The idea with this test is to excite the system when the dynamometer is in torque control mode. In this mode the dynamometer does not have a speed controller connected and the reference would be directly passed down to the frequency inverter which allows the user to specifically choose the input to the frequency inverter instead of using the output from the SC as input by for example running the BS_T_NT test described in Section 4.2. This test also is an alternative to BS_T_NT when estimating shaft parameters.

The test was designed with much focus on identifying the field oriented control due to direct access to control signal. Unfortunately the output was sampled in a

relatively slow rate. This did not allow enough precision to be able to estimate a model for the FOC. An attempt was made in Section 6.3.2 but nothing more than that the output was a low-pass filtered version of the input could be stated with certainty.

4.4 Dynamometer Torque Step Test

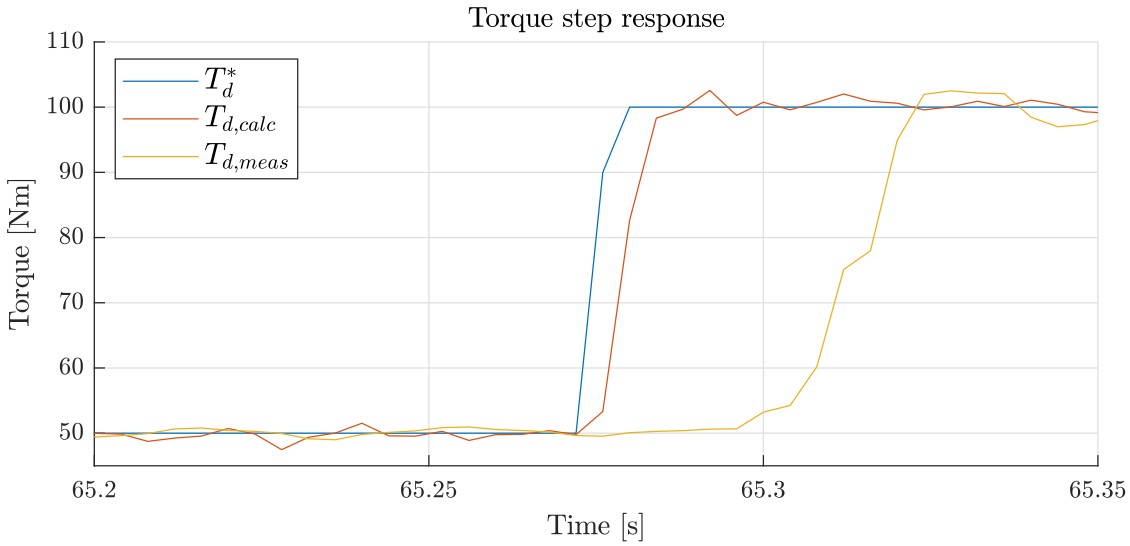

Figure 4.5: Example of step in torque obtained in experiments. The demand value T_d^* is shown together with the response in by the system calculated electromagnetic torque $T_{d,calc}$ and by the measured dito $T_{d,meas}$.

Even though single step responses rarely excite the system enough to do model parameter estimation, they can be used to show other properties such as time delay [4]. This test is mainly useful to investigate the various torque signals available in the system. By comparing these to each other and the speed one can draw conclusions about their timing. The control mode is now _T_TN.

4.5 Dynamometer Speed Ramp Test

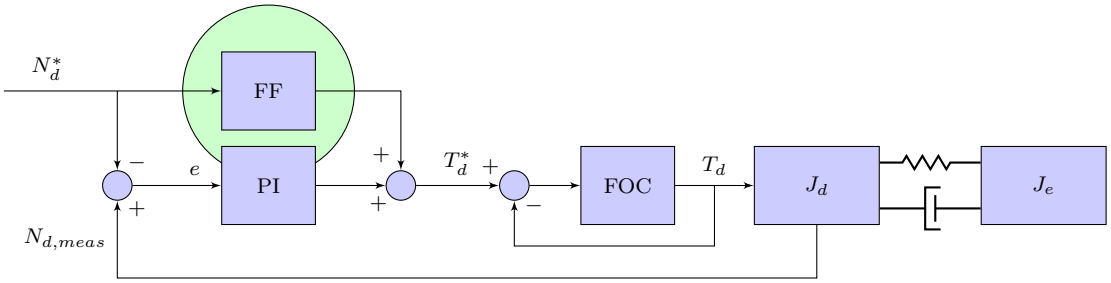

Figure 4.6: Excitation focus of this experiment is marked in green.

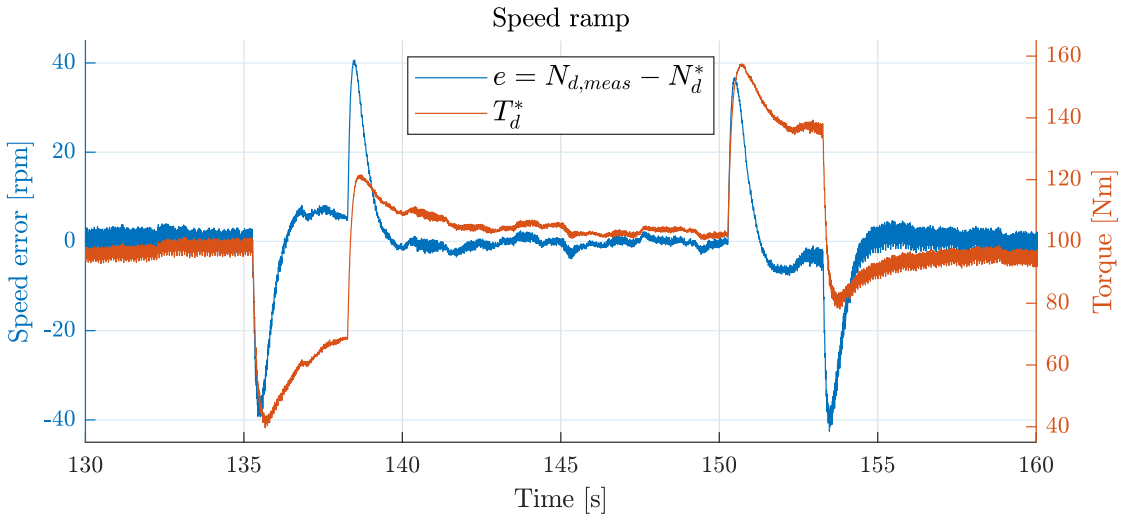

Figure 4.7: Example of speed ramp data obtained through experiment. This data is used for estimation of speed control where speed error is the input and torque demand value for FOC is the output.

This test runs on the control mode _N_NT and lets the dynamometer speed demand value N_d^* ramp from one level to another, stay there for a while and then ramp back repeatedly. The purpose of of the test was initially to analyse the system response to a change in N_d^* similar to a step response. The reason a ramp is used in place of step is to limit the torque acted out on the shaft as discussed in Section 3.3. The main utility of this test in this project turned out to be something else though. This test is the only test performed that excites the dynamometer input in speed control mode. The reasoning behind this was the fact that the speed controller was intended to be excited by a change of speed acted out by the engine. Applying this ramp data to the model (estimated by engine excited data) exposed dynamics that was not modelled (see Section 6.3.1). Thus the benefit of this test was the control mode it was run in and the signal that was excited.

4.6 Unfired Engine Test

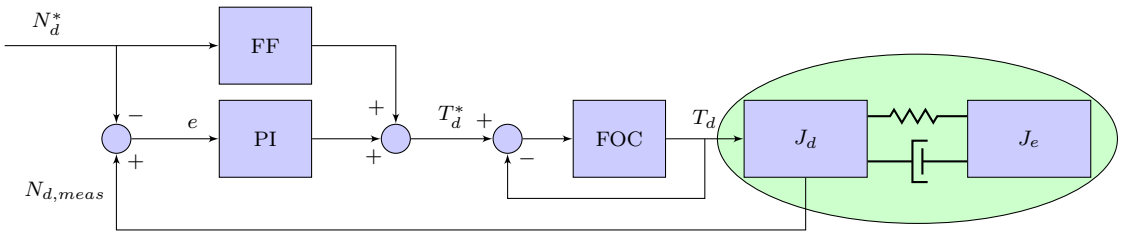

Figure 4.8: Excitation focus of this experiment is marked in green.

This test has not been performed in this project but is something that is recommended for future work. The intention with this test is to try out the method

proposed by [13] to estimate parameters for the shaft using ARMAX. Just as has been done in this project they have modelled the shaft as a mechanical two-mass system described in Section 2.4. Instead of using N_e as input due to lack of $T_{e,shaft}$ or T_e measurements they use an ARMAX structure where the engine torque can be the input of the noise model disabling the need of measurements for it.

They mention that convergent identification was not obtained using fired engine due to to large amplitude in excitation from the noise. Therefore their approach using unfired engine is proposed to try out in this experiment. The experiments would be carried out such that the dynamometer would be in speed control driving the unfired engine and excite the shaft by moving around a certain speed. This would be repeated at various speeds (operating points). System identification can then be performed for each of these levels and this would show if the spring and damping parameters are constant or varies with operating point.

Some remarks regarding this experiment follows. For two-mass identification using a ARMAX structure from T_d to N_d it is necessary to have persistent excitation on T_d to identify the dynamic model of ARMAX type. During the test it is also important that the oscillations in N_d caused by the engine inertia can be seen in the N_d data. If the engine has low inertia compared to the dynamometer it might be necessary to measure the shaft torque instead for successful parameter estimation. In the ramp data that has been performed on the dynamometer in this project it is difficult to see if this is the case because it is using a fired engine and the combustion frequency is hiding the oscillations caused by the engine inertia.

4.7 Sine Wave Reference Test

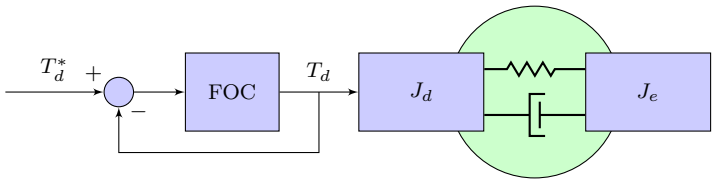

Figure 4.9: Excitation focus of this experiment is marked in green.

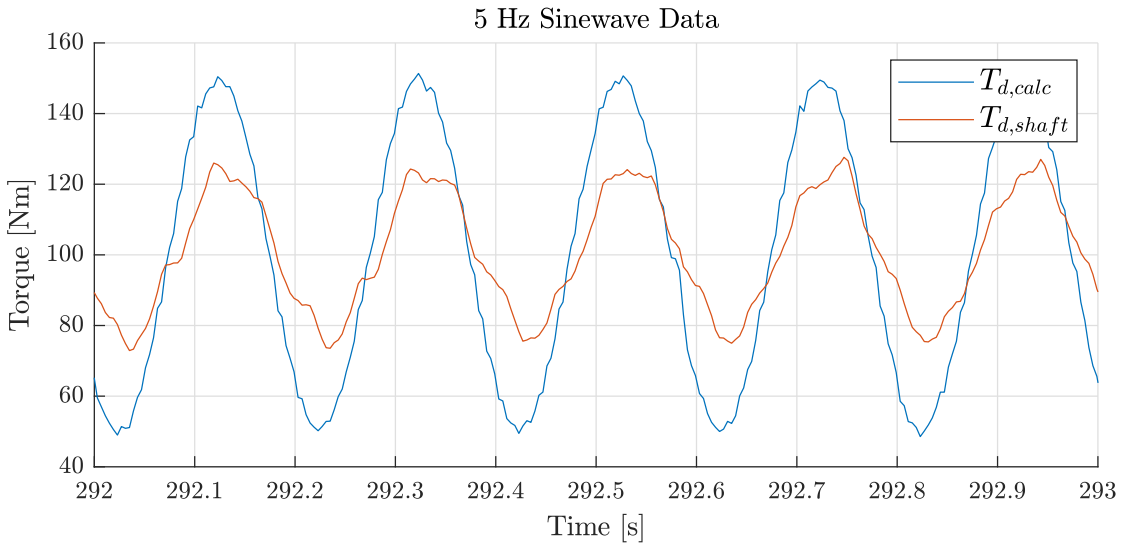

Figure 4.10: Example of sinewave data obtained through experiment. One can see that the gain from electromagnetic torque to shaft torque is less than one for this frequency.

This test was performed in T_TN control mode. The torque demand value was set to follow a set of sine waves of various frequencies one at the time. The test was designed to use sines at all integer frequencies up to 20 Hz. This experiment data can be used to analyse the gain from the input torque T_d to for example the shaft torque $T_{d,shaft}$ at the various frequencies. This can be compared to the bode gain of the transfer function for corresponding input-output at corresponding frequencies. Unfortunately the amplitude used in this test was chosen a bit to large causing system safety to stop the test due to vibrations at 18 Hz. As seen in Section 7.2 this seems to correspond to the resonance peak of corresponding bode plot. Had a lower amplitude been used then the system would have continued and data would have been gathered above the peak to see at which frequency the gain starts do drop again.

This test gave some valuable validation of the model as shown in Section 7.2. However the test could be redesigned to be improved. First of all a lower amplitude must be used and secondly it could be useful to run the test at various speeds. Perhaps the system is not linear so that the bode plot would have a different shape at different speeds. This would be due to spring-damping parameters varying with speed as was seen in [13].

4.8 Running Dynamometer Without Shaft

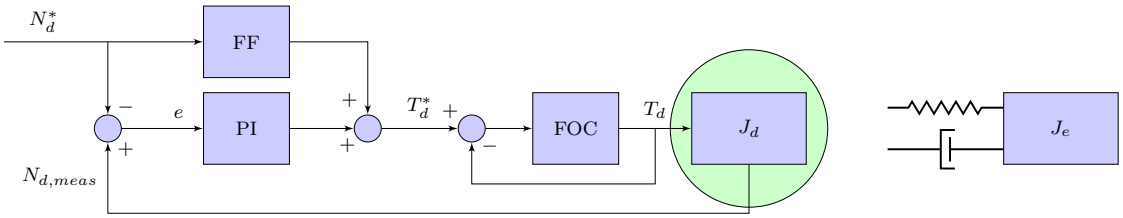

Figure 4.11: Excitation focus of this experiment marked in green.

Time did not allow for running of this test in the test bed. In this test the purpose was that the dynamometer should run without the shaft connected. Doing this would make it possible to perform a step response in dynamometer speed. The dynamometer speed could also be less limited in excitation with purpose of estimation of the speed controller SC. A third reason for running this test would be to evaluate if there is friction in the system. With the shaft disconnected the friction would be given as

$$T_{fric} = -(J_d\dot{\omega}_d + T_d) \tag{4.1}$$

with T_d defined as braking torque. This equation relies on the dynamometer being constructed such that T_{fric} is decoupled from the part of stator connected to the load cell. This is actually of importance for the system as a whole since otherwise the measurements of T_d would not be T_d but rather $T_d + T_{fric}$. In retrospect this experiment is not recommended to prioritise. This since there are more urgent experiments relating to shaft and feed forward estimation.

5
Data Analysis and Processing

This chapter starts with taking a closer look at the sampled data in the time domain, to determine if it is possible to see the effects of the combustion engine in the sampled data. It follows this study with taking a look at the data in the frequency domain to determine the general quality of the sampled data. The last part of the chapter talks about how to resample the data to get the measured signals to the same sampling rate which is necessary for system identification.

5.1 Sample Data

The signals used for system identification was sampled using sensors already present in the dynamometer system. The sampling frequency was chosen as high as possible for each type of signal and therefore different signals was sampled at different frequencies. To obtain higher sampling rate the automation system must be reconfigured to do so.

Table 5.1: A table showing the sampling frequency of each signal

Measured signal	Sampling frequency	Description
N_d	1000 Hz	Dynamometer speed
N_e	500 Hz	Combustion engine speed
$T_{d,calc}$	250 Hz	Electrical torque calculated by the dynamometer system using a mathematical model of the dynamometer
$T_{d,meas}$	250 Hz	Electrical torque measured from a torque load cell
$T_{d,shaft,calc}$	250 Hz	Torque acting on the shaft calculated by the dynamometer system from known dyno inertia and N_d

5.2 Data Analysis in Time Domain

The test object that was used during testing was a four cylinder engine which makes two combustions every motor rotation. This results in a excitation frequency of $f_{cb} = 2N_d/60$ which for the three speeds tested 1200 rpm, 3000 rpm and 4500 rpm results in frequencies of 40 Hz, 100 Hz and 150 Hz. Taking a closer look at the binary sequence (BS) data at 3000 rpm as shown in Figure 5.1, it is possible to see a

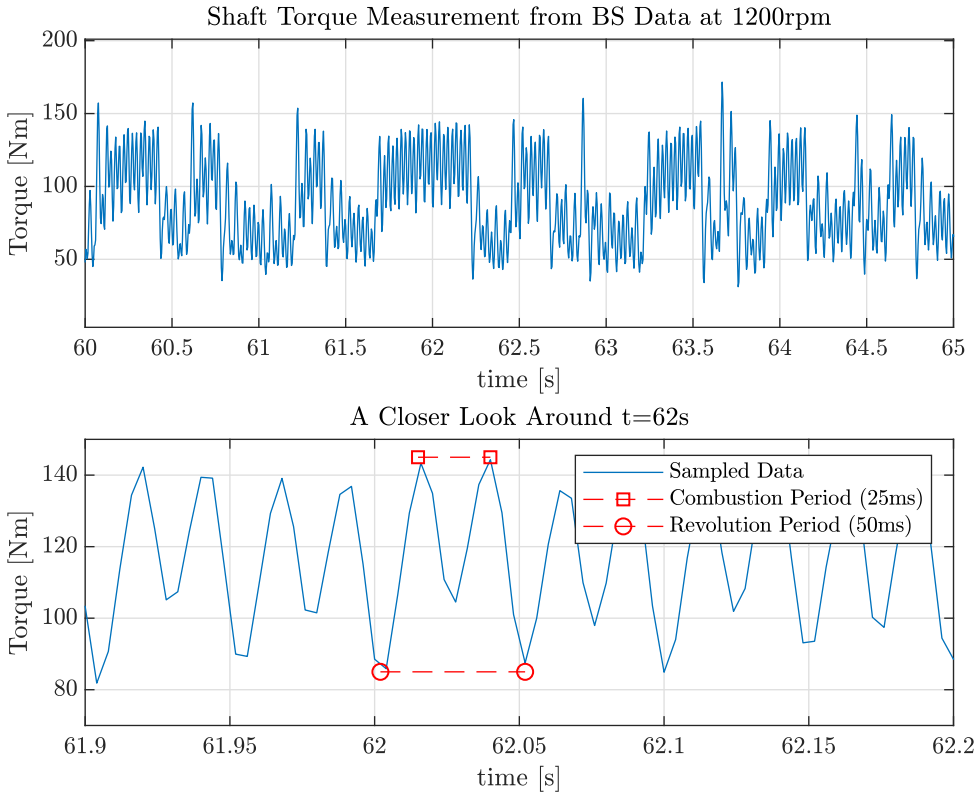

Figure 5.1: This figure is showing the effect of the engine combustions on the shaft torque. Each combustion can be easily identified by a look at the time plot and because the performance of the four cylinders aren't identical, a periodicity that fits the revolution frequency can also be found in the data. It isn't possible to see any pattern that matches the periodicity of the engine cycle.

change in the data at the combustion frequency 40 Hz combined with the frequency of rotation at 20 Hz.

5.3 Data Analysis in Frequency Domain

A good place to start when studying sampled data is to look at the spectra of the sampled data in order to find out if the frequencies close to the Nyqvist frequency have significant power or not. If the frequencies have low power at the Nyqvist frequency it is a sign that the data might be free of aliasing. Remember that the half power point is at $-3dB$ and $-20dB$ is $\frac{1}{100}$ the power of $0dB$.

5.3.1 Aliasing

At $4500rpm$ the combustion frequency is 150 Hz which is 25 Hz higher than the Nyqvist frequency at 125 Hz for T_d which is sampled at 250 Hz. This results in aliasing of the measured signal and the 150 Hz signal appears at 100 Hz in the sampled data. This has been confirmed by studying the spectrum of data collected with the BS test at $N_d = 4500rpm$ which shows that there is a power peak at 75 Hz

and 100 Hz. The peak at 75 Hz is half the combustion frequency and hence the frequency of rotation and the power peak at $100Hz$ is the combustion frequency aliased into the signal from 150 Hz.

Since the torque data collected at 4500 rpm contains aliasing it should therefore not be used for identification uncritically. Data collected at 1200 rpm has no clear indication of being subject to aliasing and is hence the best data to use for identification of models that don't require linearising at an operating point.

5.3.2 Interesting Frequency Content at 100 Hz

When running the engine at 1200 rpm the combustion frequency is 40 Hz but looking at the spectrum one can still see frequency content at 100 Hz. Some component in the system is creating these frequencies and the amplitude is large enough to affect the speed of the dynamometer which also affects the dynamometer speed controller and therefore the torque reference signal to the frequency inverter. This data is therefore present in all measurements (N_d,N_e,T_d and T_d^*).

Changing the dynamometer to torque control and sending a sampled sinusoidal reference T_d^* to the frequency inverter causes the sinusoid to appear at the same frequency as the reference T_d^*, which is to be expected. But also at $100 \pm T_d^*$, which for a sinusoid of $8Hz$ result in 8 Hz, 92 Hz and 108 Hz. The bandwidth between the automation system and the control system allows for a new reference signal every $10ms$ ($100Hz$). Because the appearance of energy around 100 Hz appears both in speed control mode and torque control mode it is likely that the dynamometer always creates this frequency. Concerning identification of FOC this means that frequency content is present in the output T_d but not in the input T_d^*. This is a typically nonlinear behaviour that needs to be taken into account if using linear models.

5.3.3 Signal Flow and Calculated Electromagnetic Torque

In the DTB test cells the electromagnetic torque T_d is calculated using a mathematical model of the system. Looking at the T_d sensor that is used for updating the model parameters one can see that there exist energy at 75 Hz as shown in Figure 5.2. Because the torque at this frequency hasn't affected the dynamometer speed N_d much as shown in Figure 5.3 it does not affect the speed controller and hence not the reference to the frequency inverter T_d^* as shown in Figure 5.4. Looking at these data and comparing it to the spectra of the calculated T_d as shown in Figure 5.5 one can see that it only contains energy at the frequencies where the torque reference T_d^* also has energy. $T_{d,calc}$ should therefore be seen as the torque that the dynamometer are trying to deliver to the system, while the measured $T_{d,meas}$ even though the sensor has it's own dynamics might be a more true to reality representation of what actually happened.

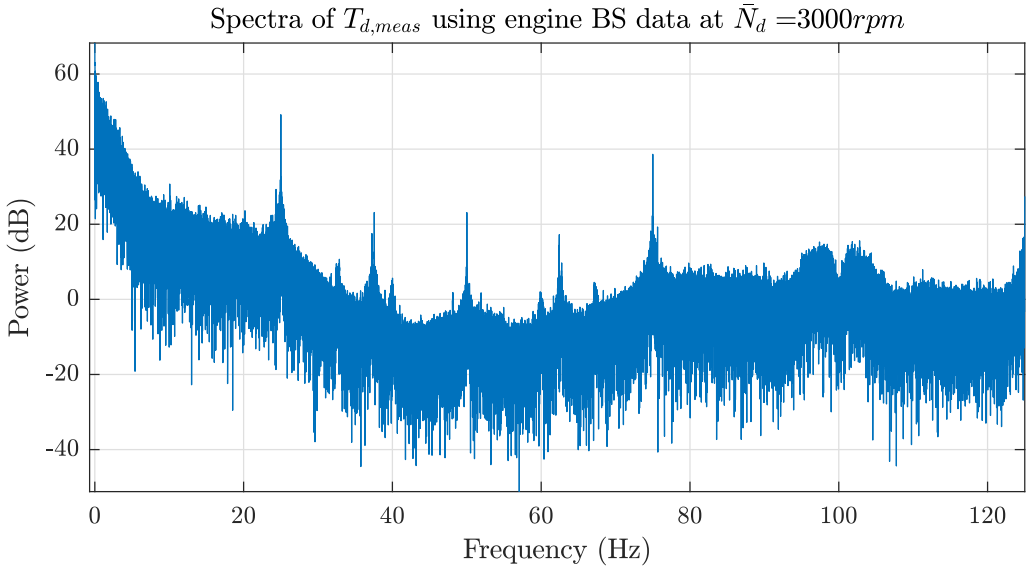

Figure 5.2: Spectra showing load cell torque measurement of the dynamometer when running a PB test at 3000 rpm. The spectra shows that the signal power is much greater at low frequencies than at high frequencies.

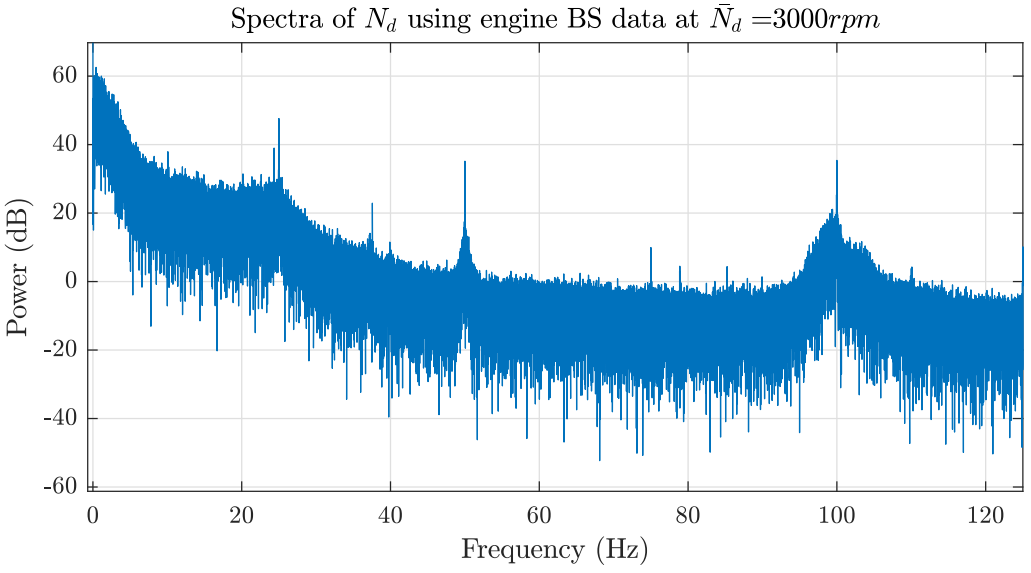

Figure 5.3: Spectra showing dynamometer speed measurement when running a BS test at 3000 rpm.

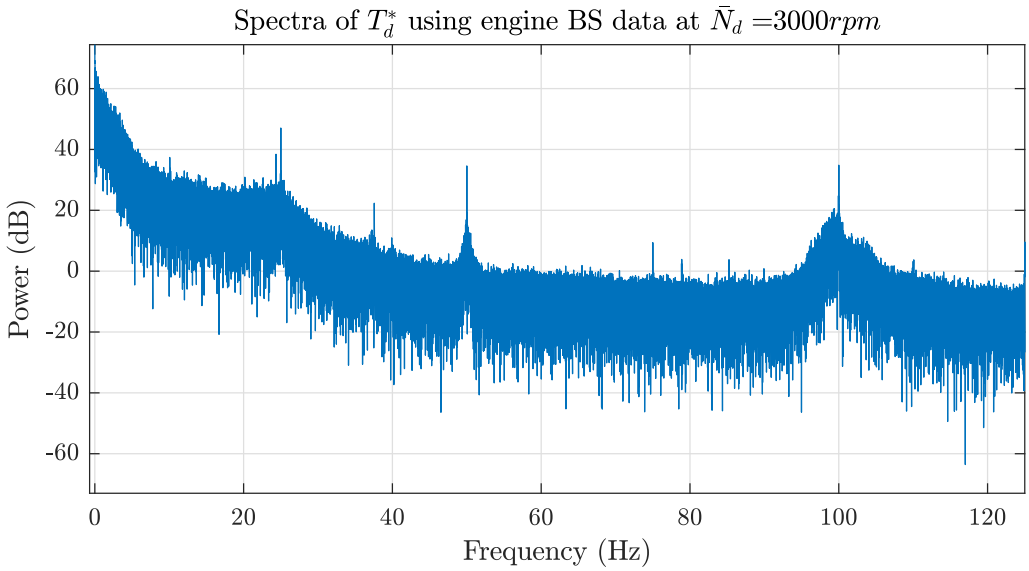

Figure 5.4: Spectra showing electromagnetic torque reference T_d^* when running a BS test at 3000 rpm.

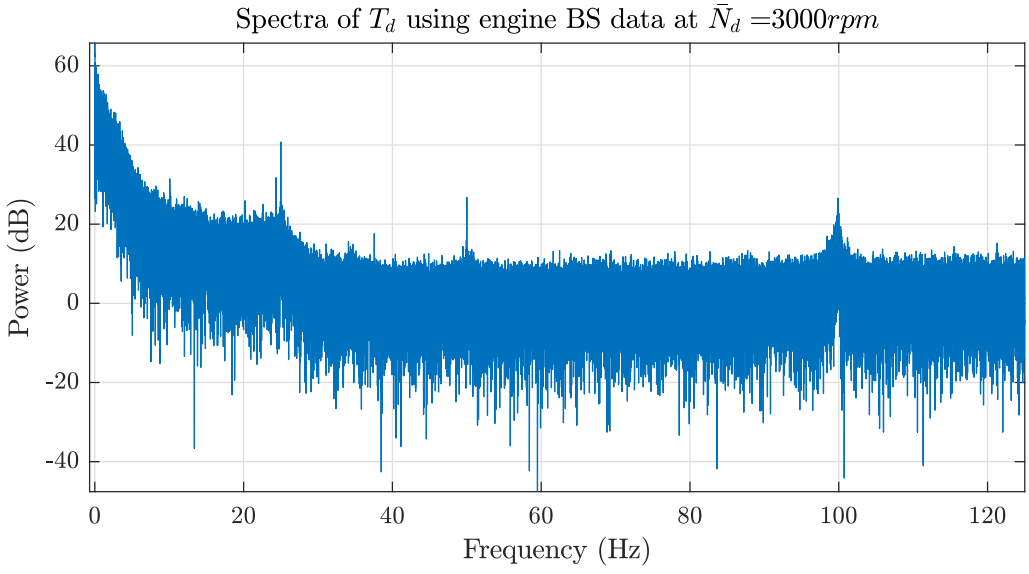

Figure 5.5: Spectra showing electromagnetic torque T_d when running a BS test at 3000 rpm.

5.4 Resampling

When estimating a system model it is necessary that the sampled input, output signals has the same start and end time and that they are sampled with the same frequency. If some signals are sampled at a higher frequency, a solution would be to use decimation to get all signals down to the same frequency. The process of decimation consists of two parts, filtering and downsampling. Where the filtering part consist of letting the signals be affected by a low-pass finite impulse response (FIR) filter and the downsampling is simply the process of removing all samples that does not match the desired frequency. It is important to note that the filtering process adds a delay to the signal which is not wanted, a solution for removing the delay is to run the data through the filter again but backwards, which removes the effect of the delay. This type of filter is called a non-causal zero-phase filter. [14]

There are many reasons why one might want to consider resampling the data before using the data for identification where the first one is to get all signals with to the same sampling rate and another reason is to get data that is more focused on low frequencies to allow for better estimation of poles and zeros in a discrete model. [14]

6
System Identification

This chapter describes modelling and system identification performed with data obtained from experiments. It begins with an analysis of signal and sensor delays in the system. This is followed by a section defining the different models that was identified. The results of the system identification procedure concludes the chapter.

6.1 Time Delays

A good initial experiment for system identification is to estimate potential time delays. Knowledge of the time delays can be useful when estimating dynamical models of the dynamometer setup. The time delays from dynamometer demand value to actuation are the most critical time delays since they limit control performance.

There are several torque values available from experiments: The by the system calculated electrical torque $T_{d,calc}$, torque measurement $T_{d,meas}$ and the calculated shaft torque $T_{d,shaft,calc}$. The first two corresponds to the air gap torque where $T_{d,calc}$ is fast and based on a mathematical model. The lever arm measurement $T_{d,meas}$ is accurate but not as fast as the calculated torque. Figure 6.1 shows a step response typical for the data obtained from experiments. When analysing the time delay in $T_{d,calc}$ one can see that it cannot be much more than 4 ms which is the sample rate. Since it is calculated one should perhaps not trust it uncritically but it is reasonable that it is significantly faster than the sensor measurement which is triggered mechanically. To get an idea of the delay of the true air gap torque T_d the dynamometer speed is evaluated as shown in Figure 6.2. One can see a sudden bending of the curve in the same time instant as the $T_{d,calc}$ follows the step. Thus it seems reasonable that the calculated torque is accurate at least in response time. The shaft torque $T_{d,shaft,calc}$ on the other hand seems to be delayed since it is increasing a few samples after the change of speed. This corresponds with what was found in Section 3.4.3 where the filtered speed introduced a delay in the $J_d\dot{\omega}$ part of $T_{d,shaft,calc}$.

To conclude this part one can say that care must be taken when using system signals for identification. The torque measurement is delayed in transient phase which makes the raw signal unsuitable for identification. The calculated shaft torque $T_{d,shaft,calc}$ is not correct in time either. On the contrary the electromagnetic torque $T_{d,calc}$ does not suffer from this at least not to the same extent. Therefore this signal is deemed more suitable for identification. Additionally the shaft torque $T_{d,shaft}$ can

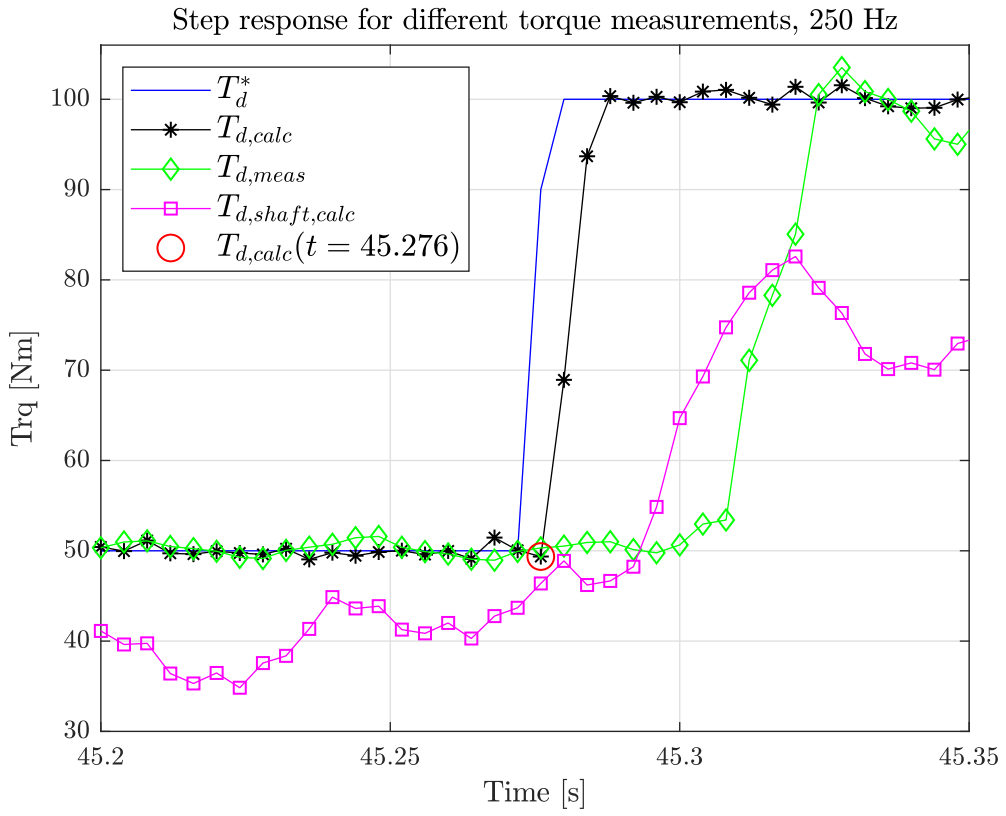

Figure 6.1: Step response in dynamometer torque for the various torque signals. These are set point T_d^*, calculated electromagnetic torque $T_{d,calc}$, measured electromagnetic torque and by the system calculated shaft torque $T_{d,shaft,calc}$. It can be seen that there is only about a sample (4 ms) delay in the calculated electromagnetic torque while the delay is longer for the mechanically measured dito. The trustworthiness of the calculated torque $T_{d,calc}$ is deemed reasonable since one can see that the speed in Figure 6.2 react in the same time instant as the calculated torque. $T_{d,shaft,calc}$ given by the system cannot be trusted as stated in Section 3.4.3 and also seen in this figure.

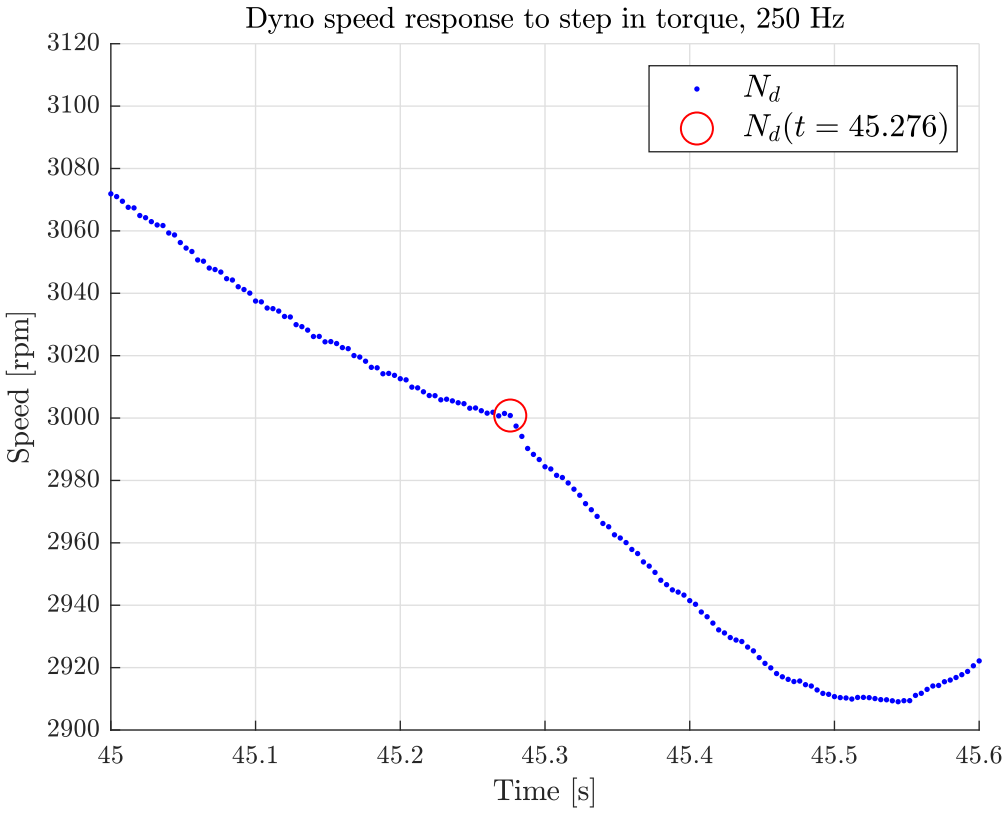

Figure 6.2: Dynamometer speed at time for a step in dynamometer braking torque. The red circle defines the time instant right before a change of torque is noticed in $T_{d,calc}$. Compare with Figure 6.1.

be calculated using this signal and zero phase filtered dynamometer speed instead of using the delayed system signal.

6.2 Modelling

The first thing to do is defining which input and output signals that should be used for the model to be estimated. The complete model must inevitably be of multiple input type (2 inputs) whereas the outputs are free to choose. The first input is the dynamometer reference value T_d^* or N_d^* and the second input would be on the engine side (see below).

Some discussion is required concerning the input on the engine side. Since this project aims to model the dynamometer and drive shaft independently of the engine this input would ideally be be either torque $T_{e,shaft}$ or speed N_e acting on the engine side of the shaft. One must keep in mind however that the model should eventually be used for simulation and by predetermining either one of those one would make the engine independent of the dynamometer. This is not an accurate description of the system. To create a sensible simulation model one thus has to take one step back and instead use T_e as the input. By doing this one unfortunately couples the engine inertia and flexibility into the model. This would make the model valid only under the assumptions that J_e is known and that the engine mechanics is stiff. If one would not like to rely on this assumption one would have to inject an additional model of the engine that takes T_e and $T_{e,shaft}$ as input and outputs N_e.

As stated above the inputs of the model are now defined. The signal flow on the dynamometer side in control mode NT is shown in Figure 6.3. This is based on the equations for the speed of the dynamometer given as

$$J_d s N_d(s)\frac{2\pi}{60} = -T_d(s) + T_{d,shaft}(s) \Leftrightarrow N_d(s) = \underbrace{\frac{60}{2\pi J_d s}}_{H_d(s)}(-T_d(s) + T_{d,shaft}(s)) \quad (6.1)$$

$$T_d^*(s) = (-N_d^*(s) + N_d(s))PI(s) + N_d^*(s)FF(s) \quad (6.2)$$

$$T_d(s) = T_d^*(s)\frac{FOC(s)}{1 + FOC(s)} \quad (6.3)$$

in the Laplace domain. PI is a feed back part of the speed controller and FF is a feed forward part. The sum of their output signals is the torque demand value T_d^*. The actual torque value T_d is then subtracted from T_d^* and this signal is passed through the FOC which again outputs T_d. In reality the FOC is more complicated and does not only control based on and output feed back. Ideally the currents should be used to model the FOC but those was not measured during experiments. Therefore this approximation is used instead to try if the FOC can be described in terms of linear black box models.

H_d outputs the dynamometer speed based on driving and loading torque. The reason

for separating the system in several submodels is because it allows for SISO- modelling. This separation is possible since both T_d and $T_{d,shaft}$ are available in DTB. The benefit of doing this is that it makes it easier to estimate them separately. In Section 6.3 the system identification of the different submodels is presented. What now follows is to add connection with the engine to the simulation model.

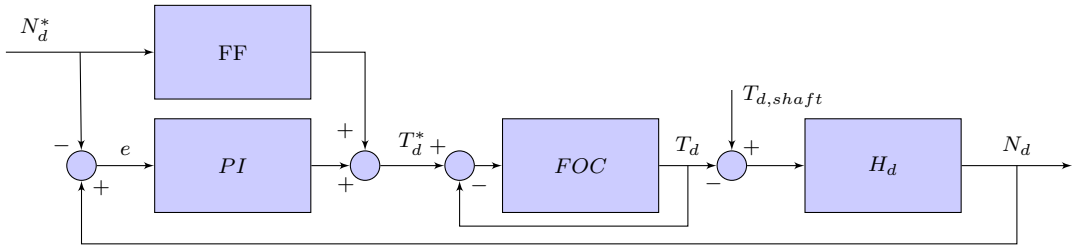

Figure 6.3: Description of the speed control of the dynamometer. The subsystem FF and PI is parts of the system speed controller while the FOC is used to create the air gap torque T_d. H_d represents how driving torque $T_{d,shaft}$ and braking torque T_d applied to the dynamometer inertia gives dynamometer speed N_d. The signs of the signals are defined to be in accordance with the measured signals in the system. Thus T_d is defined as braking torque and $N_d - N_d^*$ has been chosen to give a positive control output for a positive error signal. The representation of the FOC is an approximation made due to lack of current measurements.

The speed of the engine is obtained as

$$N_e(s) = \underbrace{\frac{60}{2\pi J_e s}}_{H_e(\mathrm{s})}(T_e(s) - T_{e,shaft}(s)), \tag{6.4}$$

in the same way as the dynamometer speed. If the shaft is modelled as a flexible shaft with internal damping as described in 2.7 it is possible to represent it as a SISO model with $N_e - N_d$ as input and $T_{d,shaft} = T_{e,shaft}$ as output and the complete model can be set together as shown in Figure 6.4. Note that this relies on the approximation of shaft inertia to be zero making the shaft torque equal on both sides. This approximation could have been avoided using an multiple input multiple output (MIMO) model of the shaft. This is not possible due to lack of $T_{e,shaft}$ measurements as described in Section 6.3.5.

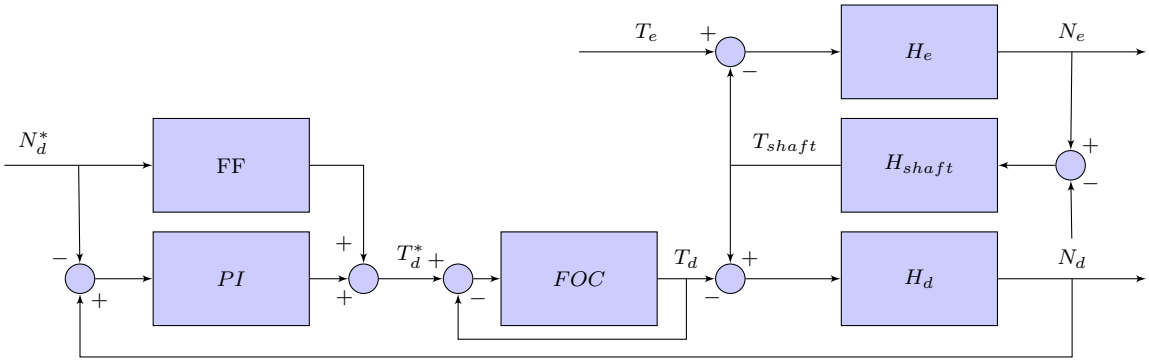

Figure 6.4: A block diagram representing the full dynamometer test bed with the shaft and engine connected. H_e and H_d includes equations from torque to speed for the engine and dynamometer respectively and H_{shaft} consists of the shaft dynamics from speed difference to shaft torque. The subsystem FF and PI is parts of the system speed controller and FOC includes the frequency inverter and the asynchronous machine excluding its inertia. FF, PI and FOC is preferably estimated on their own as SISO models but the other models could be merged together for parameter identification. Still a grey box model of a two mass oscillator would be estimated however. Therefore the model shown in this figure still would be usable for simulation because it uses the same parameters. The signs of the signals are defined to be in accordance with the measured signals in the system. Thus T_d is defined as braking torque and $N_d - N_d^*$ has been chosen to give a positive control output for a positive error signal. The representation of the FOC is an approximation made due to lack of current measurements.

6.3 Identification of Dynamometer Dynamics

In normal operation mode the dynamometer is controlling the speed. This is done by the speed controller with a control signal that is a torque demand value for the dynamometer control. This means that the torque applied to the dynamometer is controlled only indirectly. To guard against damages on the connecting shaft the torque applied to it should not exceed the torque used in normal operation. The dynamometer is able to actuate a larger torque however. This poses a limitation in the possible input signal in speed reference since the torque isn't controlled directly.

For identification purposes a white noise like excitation of the system is wanted. The limitations in sudden changes of dynamometer speed demand value poses a problem concerning the energy in excitation signal for the dynamometer. To overcome this problem an attempt to excite the system from the engine side is made instead. This is done by manually changing the ignition angle between two levels in a random manner as described in Section 4.2. This affects the speed of the dynamometer and thus excite the speed control of the dynamometer. This section is devoted to identification of the dynamometer including control system but excluding the shaft.

6.3.1 Identification of Speed Controller

To start with the identification of the feed back part PI of the speed controller follows here. It was known that there was PI- control involved in SC but not clear if this was the only thing. An attempt to estimate a pure PI- controller for the feed back part was made. It is possible to estimate the feed back part separately from the feed forward part if the BS data with constant speed demand value. That way feed forward parts proportional to the acceleration is zero and parts relating to the speed will be constant and absorbed into the estimated initial conditions of the PI- controller. The input of the PI- controller is speed error e and the output is the torque demand value T_d^* and both is sampled in 1000 Hz. From these an iddata object is created and passed into SITB for identification. Both continuous time and discrete time PI- controllers was evaluated and provided the same results. As a matter of taste the continuous time model was chosen. The continuous time PI- controller

$$PI(s) = \frac{K_p s + K_i}{s} \tag{6.5}$$

was estimated and seemed to fit the data quite well. However there seems to be an unmodelled delay corresponding to one sample in the update frequency (1000 Hz) missing. This is indicated by the fact that the simulated output very closely resembles the shape of the true output but shifted 1 ms in time. This is confirmed by the cross correlation residual plot to the left in 6.5 where there is major correlation outside the confidence region. This motivates to add a delay to the model and instead estimate

$$PI(s) = e^{-0.001s}\frac{K_p s + K_i}{s} \tag{6.6}$$

as the PI(s). Using this structure a more accurate result is obtained. Figure 6.6 shows that the simulated output using (6.6) is almost 100 % spot on. To the right in Figure 6.5 the cross correlation now is within the confidence region. Taking this altogether it seems accurate to estimate the feed back part of SC as (6.6). Given the high percentage of the fit of simulated output $\hat{T}_d^*$ it seems reasonable that the signal to noise ratio (SNR) is very low. Thus different noise realisations shouldn't affect the result to large extent and the confidence region for the model should be tight. This is indeed the case as can be seen in Figure 6.7.

Initially the hypothesis was that the speed controller did not have a feed forward part. The feed back part could very accurately describe the data with constant dynamometer speed reference. When the ramp data described in Section 4.5 was used however, the feed back part could no longer describe the data as accurately. To evaluate if this could be to properties in the ramp data an analysis was performed. This analysis is described in Section 7.1 and showed that this is not the case. Therefore the difference has instead to do with a feed forward that shows its precence when the dynamometer speed reference is non constant.

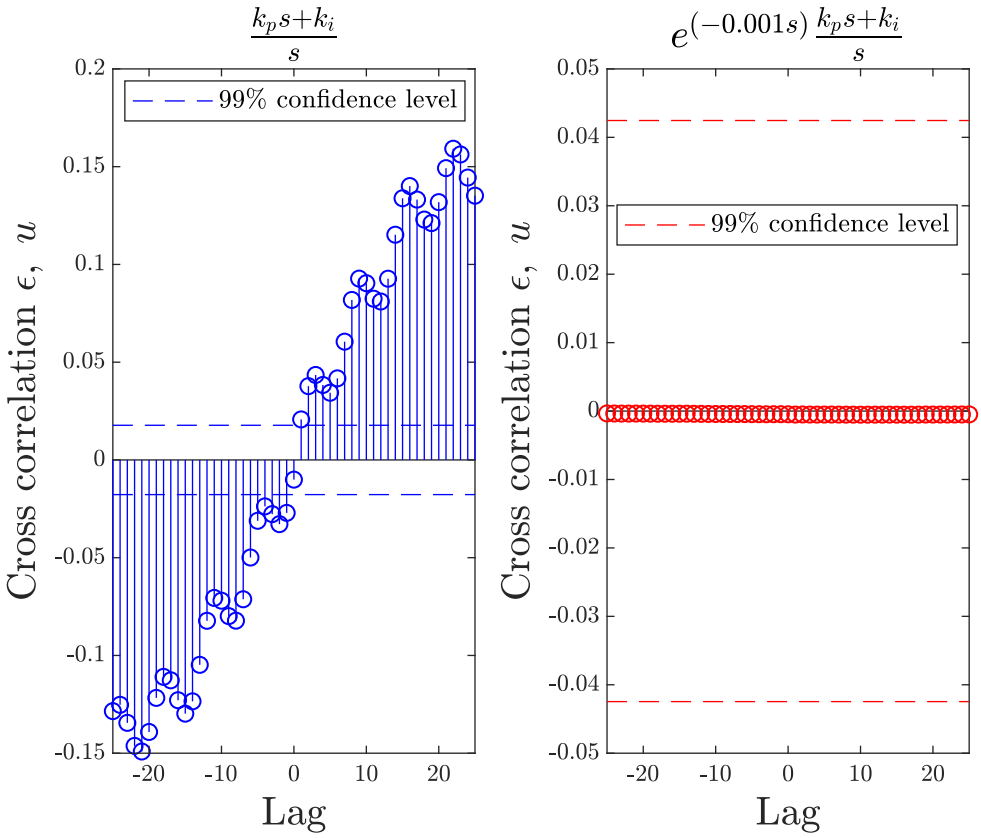

Figure 6.5: To the left is the cross correlation plot for estimated PI- controller without time delay. The correlation is far outside the confidence interval indicating that the model is insufficient to describe the dynamics applied to the input. To the right is corresponding plot for estimated PI- controller with a delay of 1 ms. This model is well within the confidence interval meaning that correlation between residual and input is statistically insignificant.

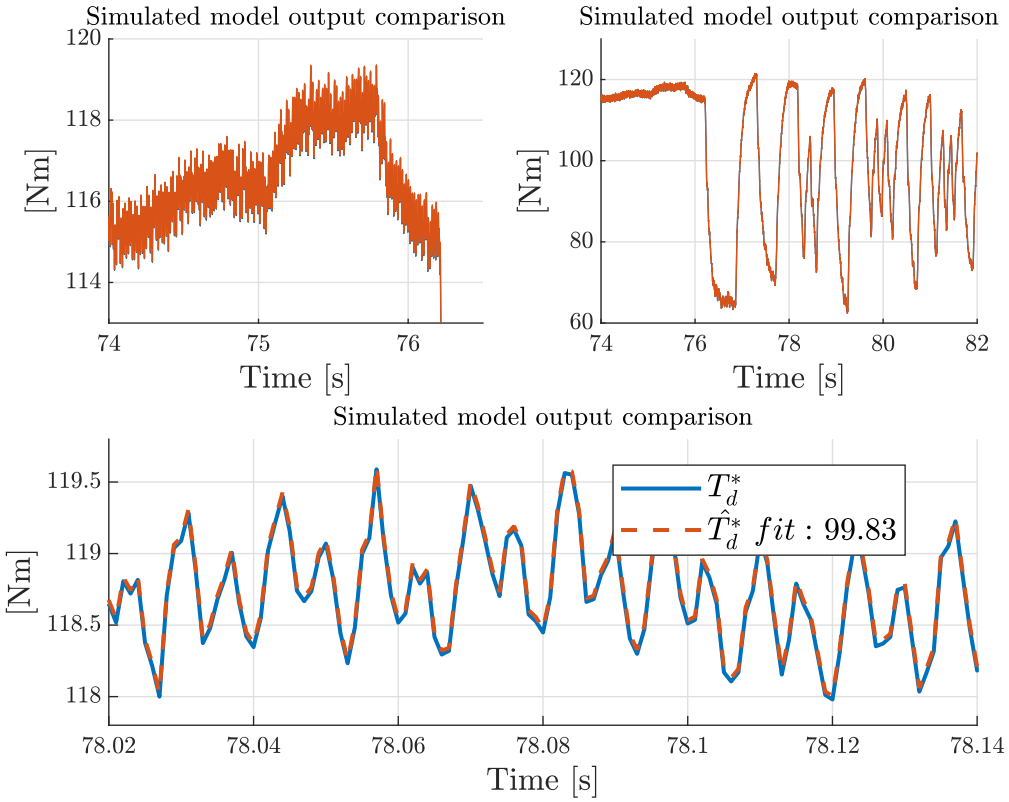

Figure 6.6: Here the comparison between simulated and measured output of the estimated PI- controller with delay is shown using validation data. The experiment is the engine excited binary sequence and the model output fits the true value accurately. The top plot shows the whole sequence while the lower plot is a zoomed in version.

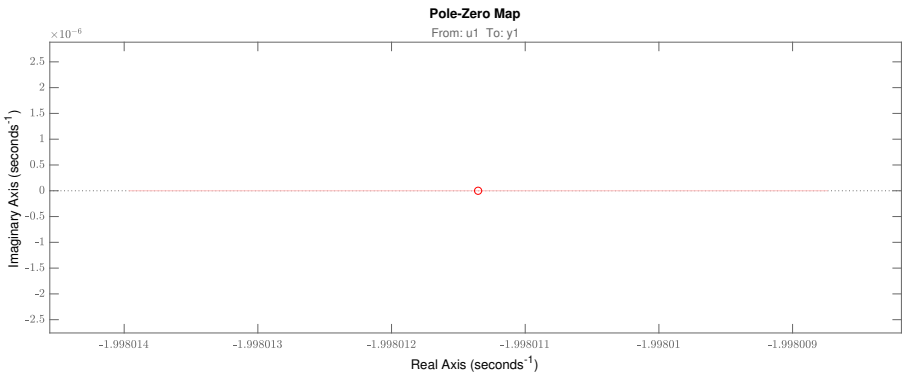

Figure 6.7: Zero placement of PI- controller defined in (6.6). The essentially noise free setting makes the confidence interval very small as seen in the figure.

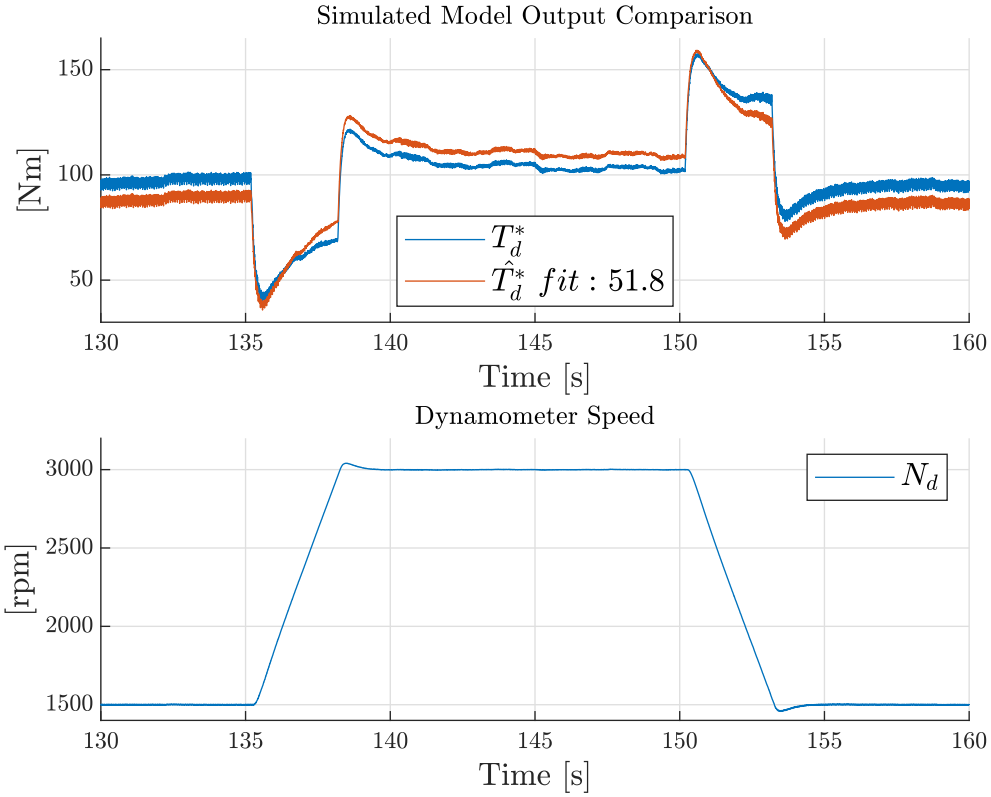

Figure 6.8: The top plot shows the model output of the PI- controller with 1 ms time delay against true output. The lower plot shows the dynamometer speed at the same time for comparison. In the top plot one can see that the model output deviates from this to large extent compared with what is seen in Figure 6.6. The difference here is that the data used is excited from the dynamometer speed reference which was constant before. One shall especially notice that the shape is similar between model output and true output except during ramping. At this time the dynamometer demand value N_d^* is non constant. This indicates that the PI-controller still is active but a feed forward has been added to the control signal.

An attempt to identify the feed forward was made. As seen previously the speed controller is operating in a relatively noise free setting. Thus an accurate value of an additive feed forward is obtained by subtracting the estimated PI- controller output from the measured output. This is shown in Figure 6.9 together with the speed demand value. It seems to be a linear relationship between the feed forward torque and the speed where

$$T_{ff}^{*} = kN_{d}^{*} + m. \tag{6.7}$$

Solving for this line using the constant levels in Figure 6.9 catches most of the feed forward term. The only deviations are where the speed is changing. By adding term proportional to the acceleration (of the demand value) these deviations are decreased. Figure 6.10 shows that using feed forward together with the PI- controller corresponds well with the measured data. To conclude it seems like the speed controller uses a feed forward term that takes both speed and acceleration into account. The former possibly is used to compensate for larger friction at higher speeds. The latter uses prior knowledge of change in demand value and is a complement to the PI- controller. This paragraph was an attempt to find a reasonable feed forward. However more investigations needs to be done in order to be confident that an accurate description of it is found. Worth noting is that the constant value m of (6.7) cannot be found definitely. This since a constant part is absorbed into the initial condition of the PI- controller and removed from the feed forward data together with the output of the PI- controller. This is not a problem for simulation purposes however where the gradient of the line is the important part.

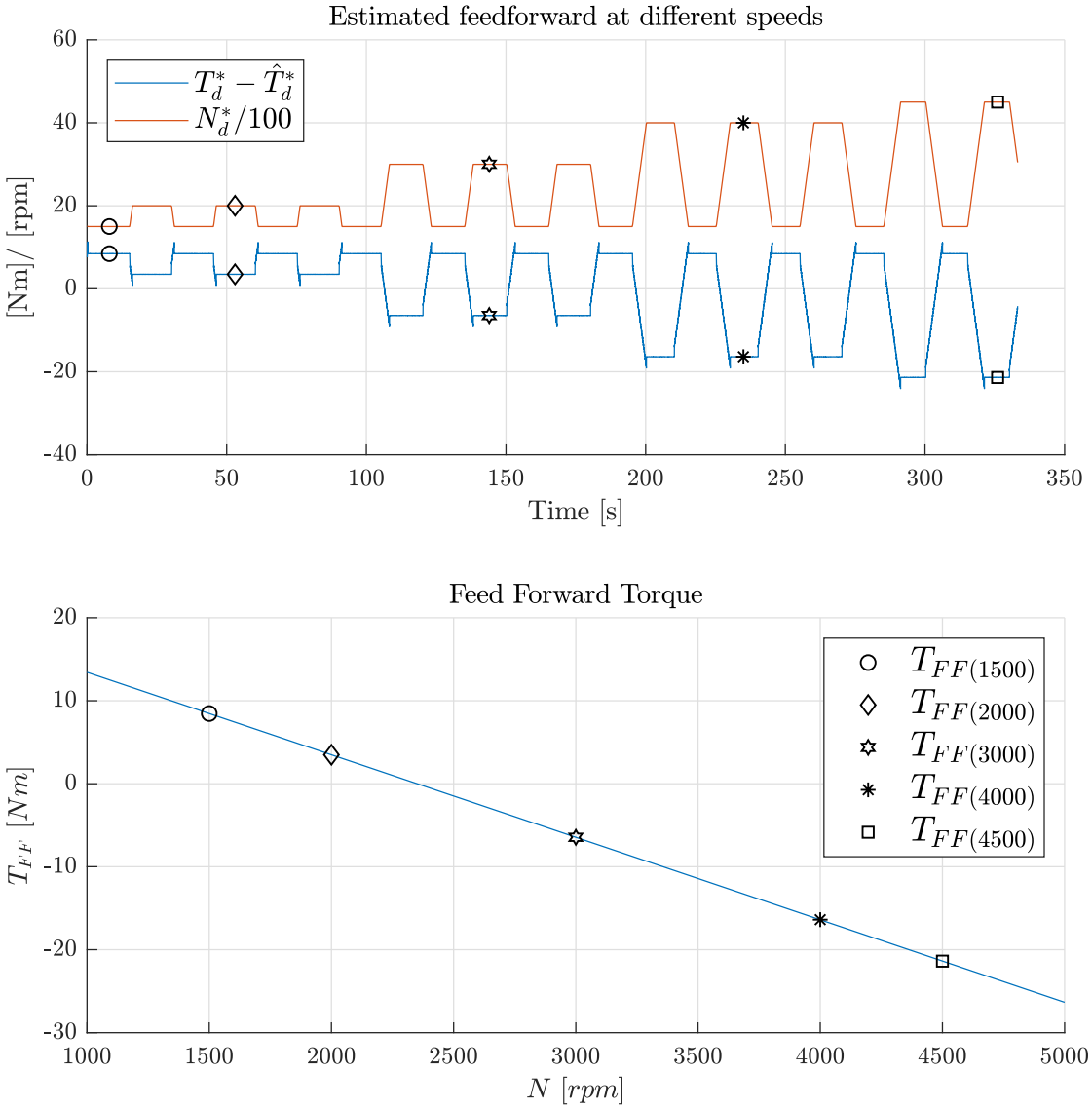

Figure 6.9: The top plot illustrates the difference between measured output and output produced by PI- controller at various speeds of ramp data (blue graph). The red graph shows the dynamometer speed reference N_d^* scaled down to fit into the plot. The two seems to have a linear relationship indicating that the feed forward term is a linear function of the speed. The marked points at the graph are mapped into the bottom graph showing the feed forward torque as a linear function of dynamometer speed.

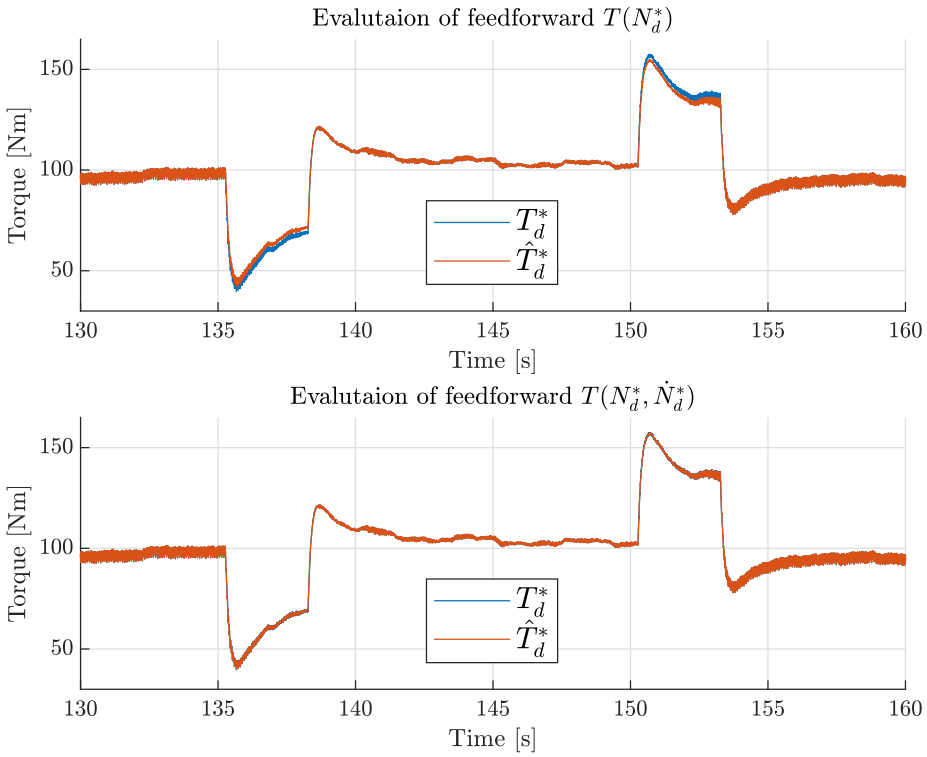

Figure 6.10: Comparison of measured output and simulated output including both PI- controller and feed forward term. In the top plot the feed forward is only a linear function of N_d^* and in the second an additional term proportional to the acceleration $\dot{N}_d^*$ has been added. One can see that the latter more closely resembles the measured data at the two peaks. These time instants is where the dynamometer accelerates and thus where the term proportional to acceleration is nonzero. The model output in this figure does more closely resemble the true output compared to not using feed forward as was seen in Figure 6.8.

6.3.2 Identification of FOC

The FOC- part consists of the frequency inverter and the electrical part of the asynchronous machine. As described in Section 2.2 this makes use of current measurements to control the electromagnetic torque T_d. From experiments in this project current measurements are however not available. Therefore an approximation of the FOC as a linear black box model using control error as input is proposed as an alternative. The possibility of this approximation is evaluated in this section. In this setting the model of FOC takes $T_d^* - T_d$ as input and T_d as output as shown in Figure 6.3. Before investigating the quality of such a black box model is evaluated an evaluation of the control performance of the FOC is made. This is done by comparing the acual torque value T_d with the demand value T_d^*.

It is a well known fact that electrical systems typically has fast dynamics. When the dynamics is fast and the output is the desired value of the input they will be similar under good control performance. Figure 6.11 shows that the output T_d indeed closely resembles the reference T_d^* but with some delay. As can be seen in the figure this delay seems to vary of about one to two samples over that data. The Matlab command *delayest* uses comparison of various ARX models to estimate the delay [15] and in this case returns estimated delay of one sample.

As shown above a pure delay can approximate the FOC relatively good, taking the low sampling frequency of 250 Hz into account. This may be used as a reference when now evaluating the quality of black box models. It is common to try out different types of linear black box models of different order to try out what seems best. Often one has some prior knowledge of especially the effect of disturbances motivating the model structure however [3]. Mainly OE- and ARX- models was investigated. Estimation data used was white noise torque excitation from the dynamometer while engine was controlling the speed. Different orders of the models was tried out. One should generally choose the model order high enough to enable flexibility enough to explain the output data. If one chooses an order too high however the model may get to flexible so that it starts to model noise. A model that has its zeros and poles located with significant distance apart from each other typically describes important dynamics. If a pole and a zero is located close to each other on the other hand more detailed dynamics is modelled which may indicate noise modelling. Figure 6.12 shows the the pole- zero map for some of the estimated models. According to previous reasoning the low order model of ARX and OE is to prefer of the models shown in the figure.

The simulated output comparison for the above mentioned low order models is shown in Figure 6.13 and 6.14. Figure 6.13 is showing validation of the same type as estimation data, i.e. dynamometer excited white noise torque. Figure 6.14 on the other hand shows validation data of engine excited torque data. One can see that the OE model performs better than the ARX model when the excitation is from the dynamometer (FOC) side in Figure 6.13. When the excitation is comming from the

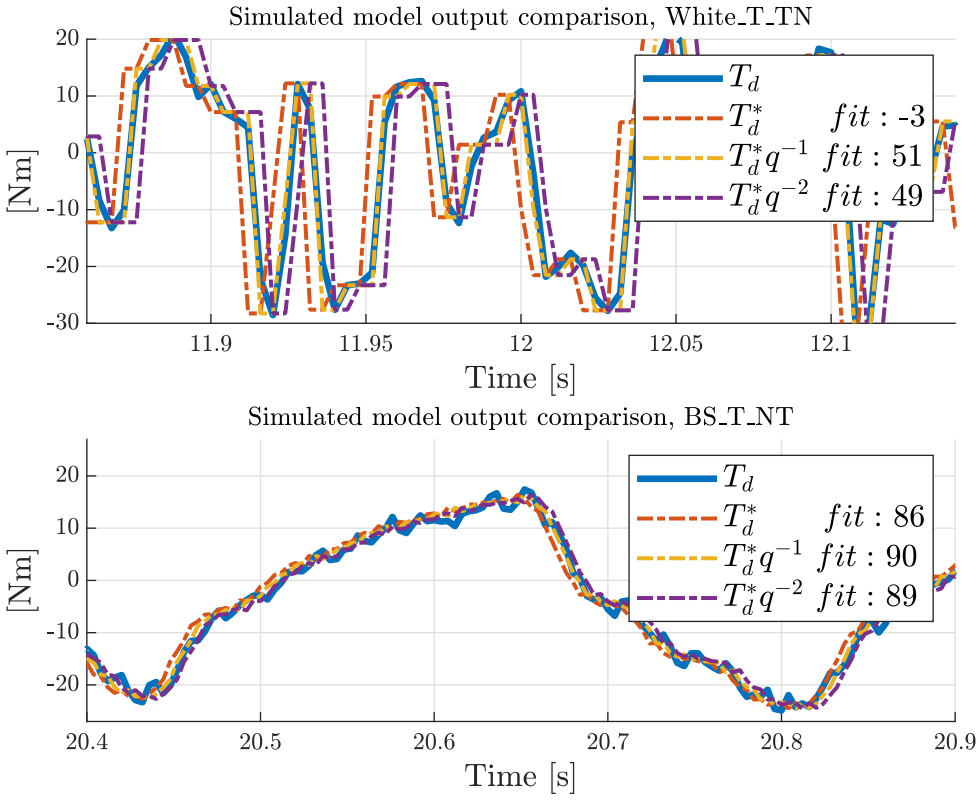

Figure 6.11: This figure shows how well delayed versions of the dynamometer torque reference value T_d^* represents T_d as the output of the FOC. The dynamics of the FOC is very fast since the output closely resembles the input. As can be seen different amount of delay matches best throughout the data sets. The delay varies between one or two samples throughout the data set.

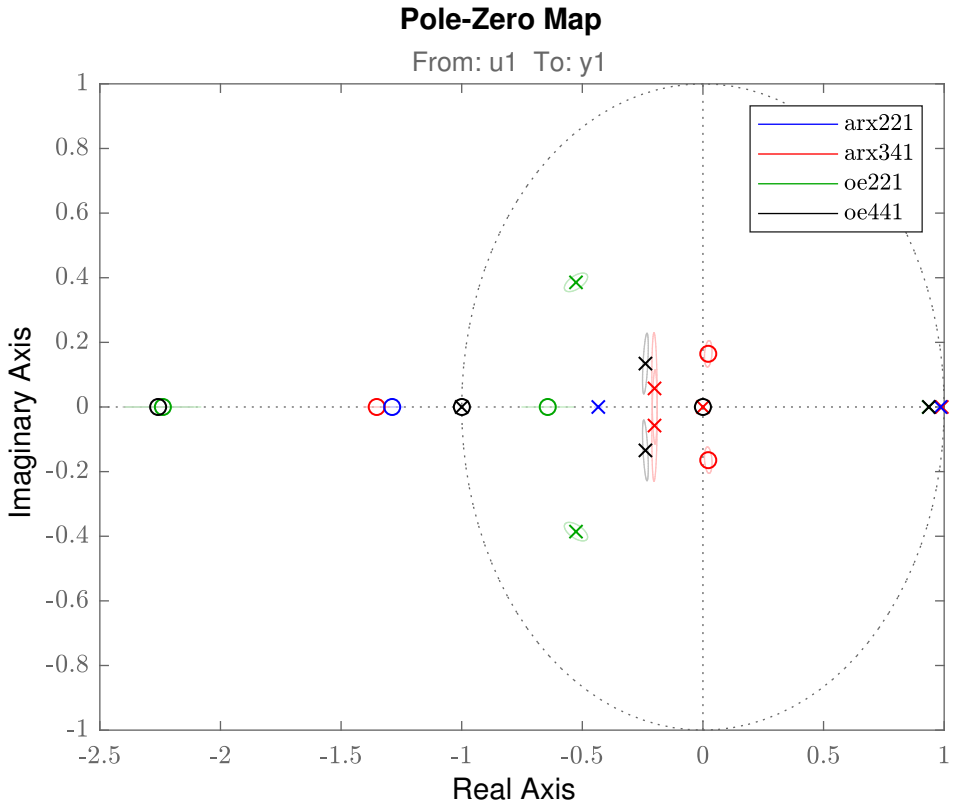

Figure 6.12: Pole-zero map of various black box models of ARX and OE type aimed to model the FOC submodel. Models of various orders (number of parameters) was tried out. The lower order models shown here is of order large enough to give flexibility to explain input-output data. However they still are of order low enough to make use of all parameters. This means that they do not place poles and zeros very close to each other which would essentially cancel out their effect. To large of a model order would also let the model tune itself towards the specific noise realisation in the estimation data. One can see that the higher order models has larger uncertainty in the pole placement and is thus sensitive to different noise realisations.

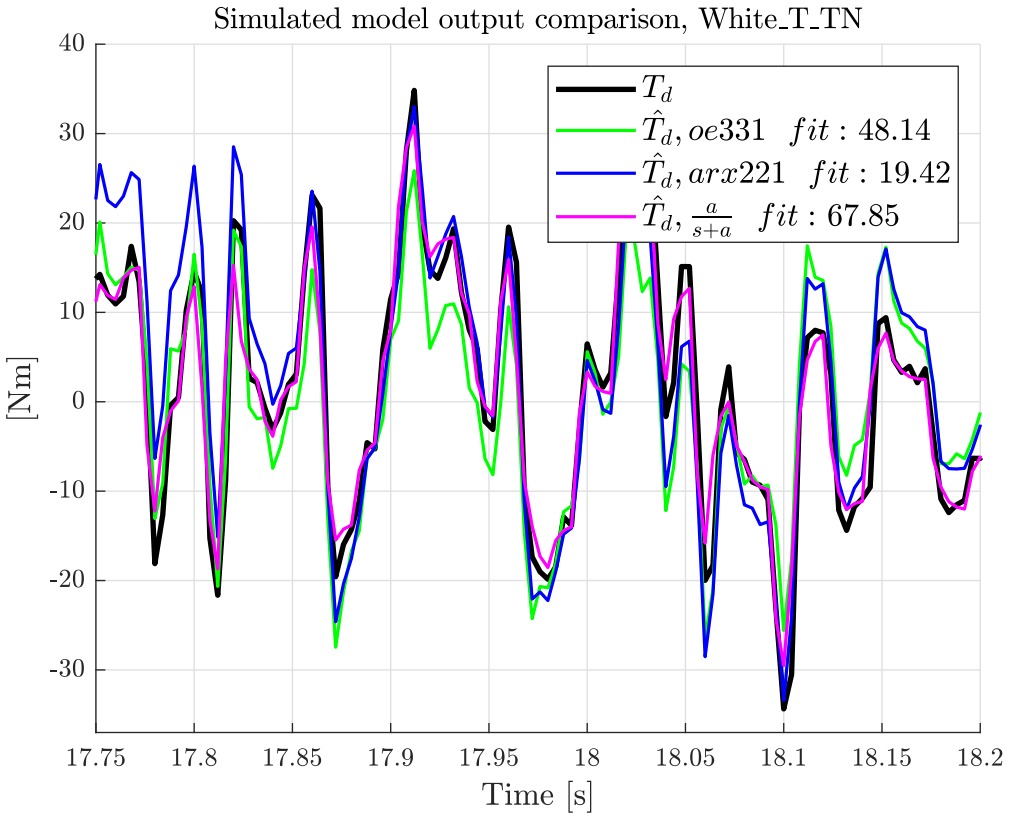

Figure 6.13: This figure shows how well the black box models can simulate the output of the FOC for dynamometer white noise data. In this data the excitation is coming in torque demand value from the dynamometer and one can see that the OE- model performs better than the ARX- model which makes use of a noise model. This noise model is however useful when the excitation is coming from the engine side as the ARX- model performs better in engine excited data as seen in Figure 6.14. A lowpass model with the torque demand value T_d^* as input is also plotted as a reference for the performance of the black box models. With respect to this one can see that even the OE- model performs poorly.

engine side however the ARX model is better. This may be because a noise model can help to explain the torque disturbances caused by the combustion engine.

One thing is worth noting when looking into previous described figures, and that is that none of the black box models performs good enough. Compared to the pure delay of demand value shown in Figure 6.11 the linear black box models performs poorly. The best description of the FOC turned out to be a lowpass model (with T_d^* as input) on the form $\frac{a}{s+a}$. This model is also included in Figure 6.13 and 6.14.

The conclusion drawn here is that the FOC indeed has fast dynamics and is able to actuate the demand value quite accurately. The estimated linear black box models could not describe the dynamics of the FOC well since they performed worse than

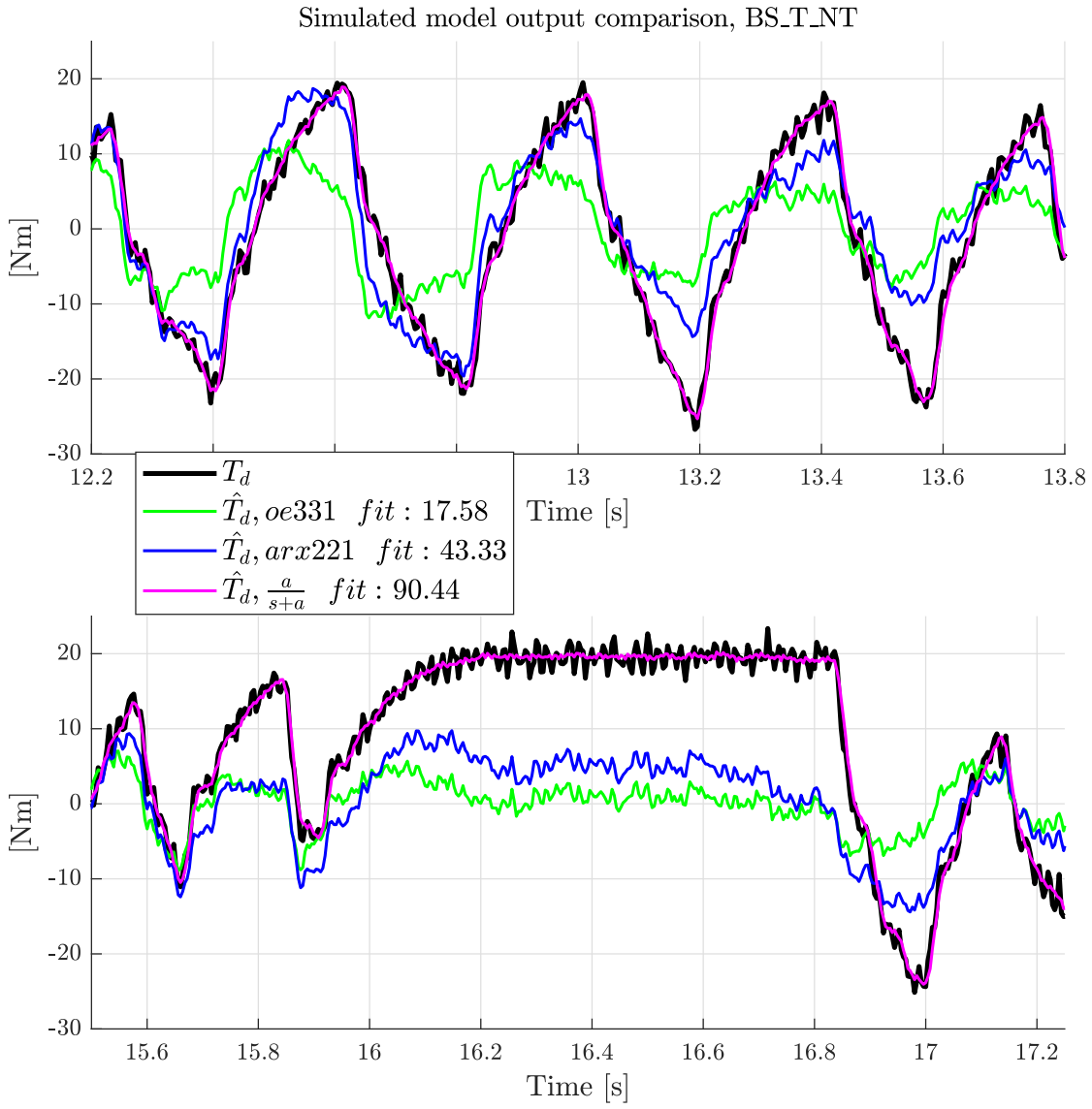

Figure 6.14: This plot shows how well the black box models performs for the engine excited binary sequence data. Here the ARX- model performs better than the OE-model since the excitation is coming from the engine. Thus it is reasonable that the ARX- model makes use of its noise model to handle this. However the performance of the black box models is poor comparing to the third model in the figure. That is a lowpass model taking torque demand value T_d^* as input. The black box models has difficulties to explain the steady state torque. This is a major disadvantage since low frequency content should be modelled accurately for a controller.

a delayed version of the input. Possibly better models could have been obtained if the sample rate had been higher than 250 Hz. Either way the control performance of the FOC is fast and accurate compared to the shaft- and speed control- model. Therefore the choice was made to remove the FOC model from the evaluation of the complete system, i.e. approximating the actual torque T_d with the demand value T_d^*. The expression for T_d in (6.3) then simplifies to

$$T_d(s) = T_d^*(s) \tag{6.8}$$

This is what was used in the analysis described in Chapter 7.

6.3.3 Submodel H_d Defined by Dynamometer Inertia

The submodel H_d in shown in Figure 6.3 is analytically defined by (6.1) with the dynamometer inertia J_d as only parameter. The value of J_d can be obtained from the product specification for the dynamometer. In the SISO setting this must be taken as a given and cannot be estimated since part of the input $T_{d,shaft}$ is calculated based on J_d and not measured.

6.3.4 Submodel H_e Defined by Engine Inertia

The submodel H_e is the engine equivalent of H_d described in Section 6.3.3. The only parameter of the model is thus the engine inertia J_e. The value of J_e is used in the analysis of the model in Chapter 7. The value that has been used is taken from what is parameterised in the automation system. However the same value is parameterised for several different engines so it might deviate to some extent from the value of the actual engine used. However J_e is not used in system identification in this project. In the analysis of the complete system (see Chapter 7) the use of J_e is necessary. The value given in the automation system is then assumed to be close to the true value.

6.3.5 Identification of Shaft Dynamics

This section introduces various approaches for estimating a parameterised model of the shaft. It begins with describing the black box identification procedure that is expected to give the best results, but isn't identified in this thesis because experiments weren't performed that allows for good estimation of this model structure. This is followed by a second model, that was identified, and is a grey box model of the shaft that is created with the purpose of allowing for all submodels to be connected.

System identification requires that measurements for all inputs and outputs are available which also affects what model structures that are possible to identify. Figure 6.15 shows a SISO model created with the assumption that the inertia of the shaft is neglectable which results in that $|T_{d,shaft}| = |T_{e,shaft}|$ and therefore one output T_{shaft} is enough. The benefit with using this model structure is simplicity and the fact that both input and output signals are available. The second model in

Figure 6.15 is a MIMO representation of the shaft which allows for the shaft to have inertia included which increases the complexity by allowing $|T_{d,shaft}| \neq |T_{e,shaft}|$. The benefit of using this structure is that it doesn't make the assumption that the shaft inertia is zero and is therefore a more true to reality model. The negative with this model structure is that $T_{e,shaft}$ isn't a signal that is measured by the system and therefore isn't available for study in this thesis. This results in the limitation that only SISO models with less complexity compared to MIMO is possible for models that only include the shaft. The alternative as mentioned above is to identify a larger black box model including the mechanical components of the dynamometer, engine and shaft which is expected to give the best results.

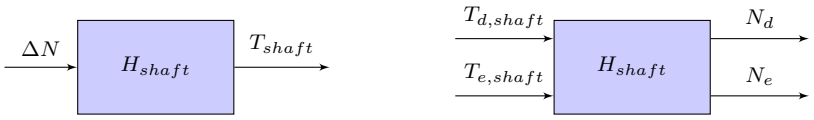

Figure 6.15: This figure shows two possible structures for modelling the shaft. To the left is a SISO model with speed difference $\Delta N = N_e - N_d$ as input and T_{shaft} as output. This model assumes that the inertia of the shaft is zero which allows the torque to be the same at both sides of the shaft. The model to the right is a MIMO and does not make this assumption and therefore has two outputs. The inputs are the shaft torque on the dynamometer side $T_{d,shaft}$ and combustion engine side $T_{e,shaft}$.

6.3.5.1 Black Box Model of Two-Mass System

A model of a dynamical system can be used for simulation, controller design, system analysis and so on. How the model should be parameterised depends on what the model shall be used for. In this case the desired structure is a white box where, the inputs are T_d and T_e and the outputs are N_d, N_e and T_{shaft}. The described structure corresponds to a white state space where the structure is known. This structure can however not be identified because one of the inputs T_e is not measured. It is however possible to identify the system by considering T_e as a disturbance while identifying the SISO system from T_d to N_d. The performance of this structure has already been studied by other people as mentioned in Section 2.4. The procedure as described in [13] is stated to have been successful (in simulation) for a noise excitation of up to half the excitation of the input T_d before it fails. They have also verified that their method works on a physical dynamometer test bench.

No experiment has been made in this thesis that fulfils this criteria and the identification has therefore given very poor results. The recommendation for the next step in the identification procedure is to perform a new experiment where the dynamometer is in speed control mode and changes the speed reference value for the purpose of having rich and persistent excitation of T_d. In [13] they also performed the experiment with an unfired engine which is recommended to try if possible. However identification using a throttle angle $\alpha = 0$ might still be possible if enough excitation can be delivered to T_d though it is unnecessary to use this more aggressive approach, if running with unfired engine is possible.

The ARMAX identification process is discrete and the continuous system that was introduced in Section 2.4 needs to be discretised before identification. The resulting discrete MIMO system (6.9) has common poles $A(q^{-1})$ for each input but different zeros from each input to each output. It turns out that $G_{11}(q^{-1}) = B_{11}(q^{-1})/A(q^{-1})$ contains all the system parameters which can be extracted from the coefficients of $G_{11}(q^{-1})$. The calculation of the order that should be chosen for the ARMAX structure depend on how the engine nonlinear friction is modelled, see [13] for the derivation.

$$A(q^{-1}) \begin{bmatrix} \omega_d \\ \omega_e \end{bmatrix} = \begin{bmatrix} B_{11}(q^{-1}) & B_{12}(q^{-1}) \\ B_{21}(q^{-1}) & B_{22}(q^{-1}) \end{bmatrix} \begin{bmatrix} T_d \\ T_e \end{bmatrix} \tag{6.9}$$

6.3.5.2 Shaft Modelled as a Gray Box Transfer Function

A grey box model is built based on knowledge of the physical model. The shaft connecting the dynamometer with the combustion engine has a pretty complex geometric shape and consist of various types of materials along its body. The gray box model studied in this section approximates the shaft to be a weak axle with internal dampening [11] and focuses on modelling the vibration dampening properties of the shaft.

The shaft is approximated as a weightless flexible cylinder that connects the dynamometer with the engine resulting in a two mass oscillator system as shown in Figure 3.6. The transfer function considered here uses the difference in speed $\Delta\omega = \omega_e - \omega_d$ as input and the shaft torque T_{shaft} as the output. The shaft is modelled using equation $T_{shaft}(t) = K \int \Delta\omega(t)dt + B\Delta\omega(t)$ where K is the spring constant of the shaft and B is the damper constant. Following up with the Laplace transform gives the system

$$\frac{T_{shaft}(s)}{\Delta\omega(s)} = \frac{K + Bs}{s}, \tag{6.10}$$

which is the transfer function structure that is be used for gray box modelling. In Figure 3.6 the spring and damping of the shaft is simplified down to one spring and damper. In the real drive shaft this would be a combination of the flex of the metal and rubber parts of the drive shaft. The transfer function (6.10) was estimated in SITB using engine binary sequence data at 1200rpm, with $T_{d,shaft}$ calculated from N_d and $T_{d,calc}$. This resulted in a prediction performance as shown in Figure 6.16. When estimating the transfer function on unfiltered data, the zero is placed between the two shown in 6.16. The prediction performance is also worse compared to the model estimated on high frequencies.

The transfer function shown in Figure 6.17 are very sensitive to the estimation data and the confidence region for the zero placement are within the region $-550 < zero < -300$ which is a very large region.

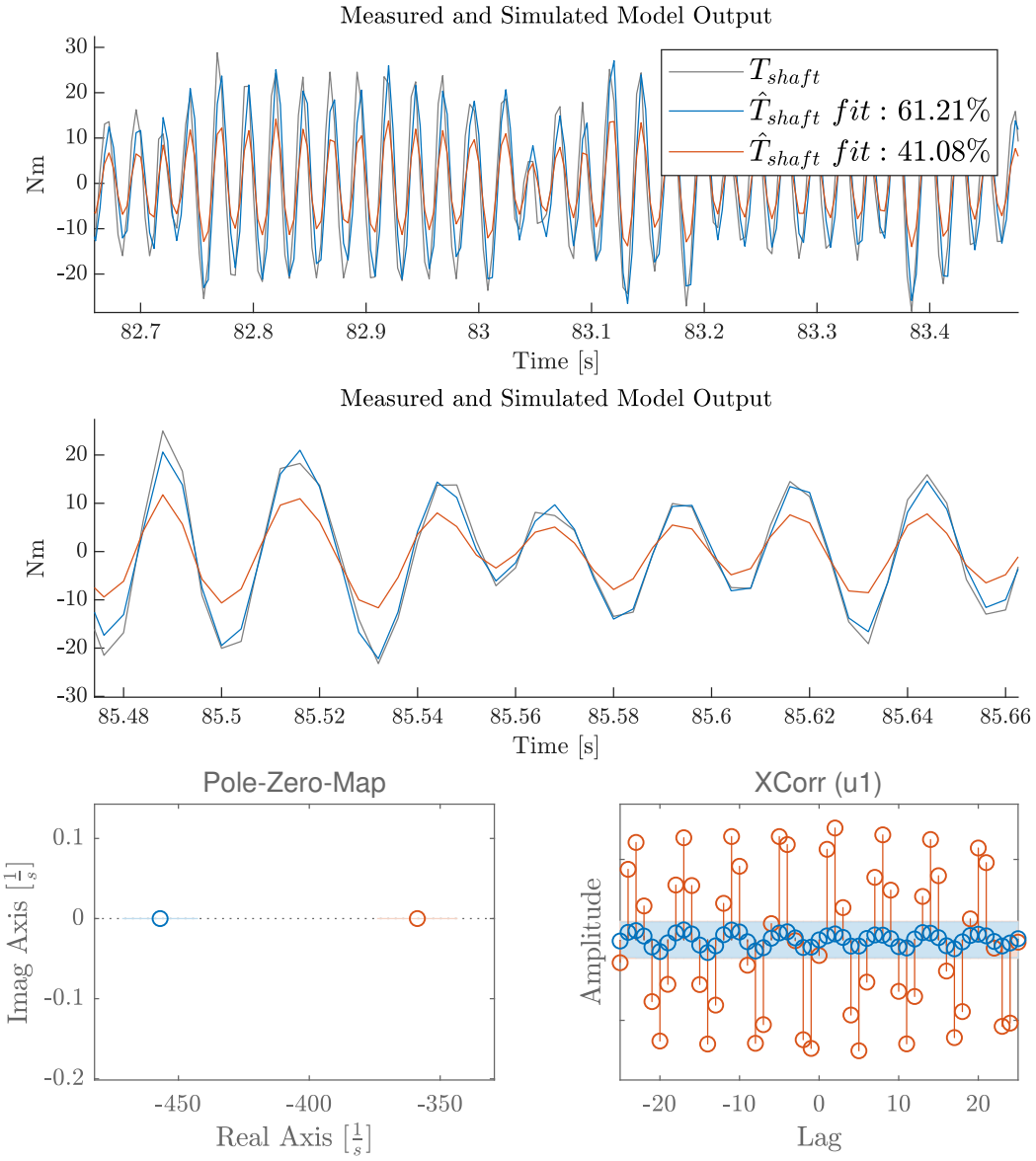

Figure 6.16: This figure shows the performance of the grey box transfer function model for the shaft when estimated to focus on frequencies higher or lower than $30Hz$. $\hat{T}_{shaft}$ shows the simulated performance of the estimated model and T_{shaft} has been calculated using $\dot{N}_d$ and T_d. The data used in this experiment is binary sequence data from the engine running at $1200rpm$ (combustion frequency of $40Hz$). The first model (blue) is estimated using high pass filtered data with the half power point ($3dB$) set at $30Hz$ while the second model (orange) is estimated using data low pass filtered at $30Hz$. The validation data is high pass filtered with half power point at $30Hz$. In this figure one can see that the model that is estimated on only the high frequencies have a higher gain and is able to predict the torque at these frequencies.

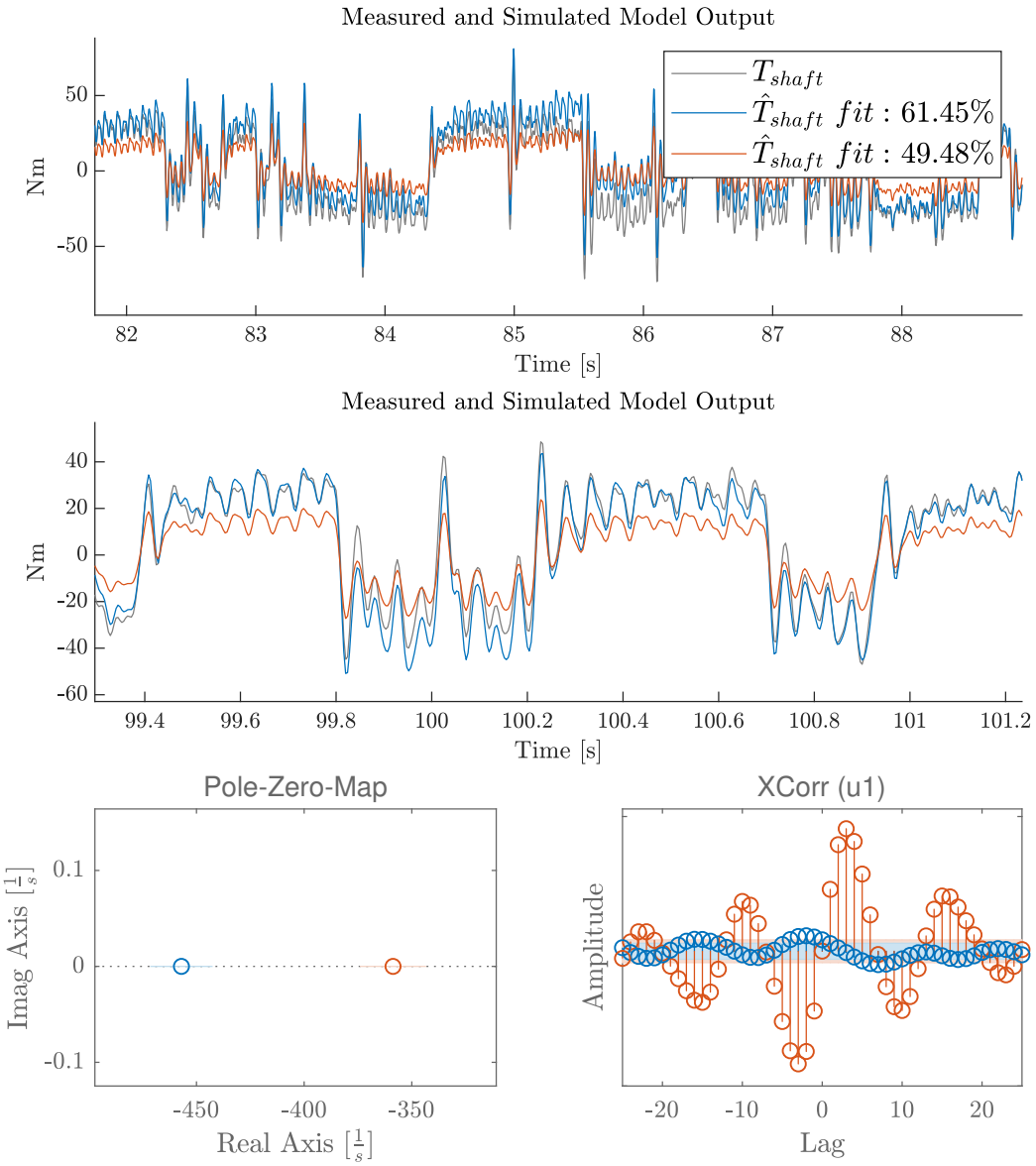

Figure 6.17: This figure shows the same models of the shaft as Figure 6.16 with the difference that the validation data now is low pass filtered at $30Hz$. The thing to note from this figure is that the model estimated using high pass data still outperforms the the model that has focuses on these frequencies. When estimating on unfiltered data the zero is placed in between the zero of these two models and it still performs worse than the model estimated on high frequencies.

6.3.5.3 Shaft Modelled as a Gray Box State Space with Known Inertia

The shaft can also be modelled as a second order state space with electromagnetic torque T_d and the combustion engine speed ω_e as input. Using the equation for the dynamometer inertia $J_d\dot{\omega}_d(t) = T_{shaft}(t) - T_d(t)$ and the shaft equation $T_{shaft}(t) = K\int \Delta\omega(t)dt + B\Delta\omega(t)$ result in the following state space where $\omega_d(t) = 2\pi N_d(t)/60$.

$$\begin{aligned} \begin{bmatrix} \dot{\omega}_d \\ \Delta\dot{\theta} \end{bmatrix} &= \begin{bmatrix} \frac{-B}{J_d} & \frac{-K}{J_d} \\ 1 & 0 \end{bmatrix} \begin{bmatrix} \omega_d \\ \Delta\theta \end{bmatrix} + \begin{bmatrix} \frac{-1}{J_d} & \frac{B}{J_d} \\ 0 & -1 \end{bmatrix} \begin{bmatrix} T_d \\ \omega_e \end{bmatrix} \\ \omega_d &= \begin{bmatrix} 1 & 0 \end{bmatrix} \begin{bmatrix} \omega_d \\ \Delta\theta \end{bmatrix} \end{aligned} \tag{6.11}$$

which contains the dynamometer inertia J_d and the shaft spring constant K and shaft damper constant B. This model structure does not need $T_{d,shaft}$ and hence the dynamometer acceleration does not need to be calculated when using this model structure. J_d still needs to be known when using this model just as in the previous model.

7
Analysis

7.1 Simulate PI- Controller Using Ramp Data

As seen in Section 6.3.1 a seemingly accurate model of a PI- controller for engine side excited data (in T_NT control mode) fails to accurate predict dynamometer excited data (in N_NT control mode). This section describes simulations aiming to find out if this inaccuracy could be explained by the properties in input data. If this is not possible the modelling of SC as a pure PI- controller must be rejected. As was noticed when using engine excited data there seems to be zero noise present. The output of the SC is a digital signal which should be noise free. The input is not accessible directly but calculated from measured data of N_d and N_d^*. However these are sampled in the same frequency $1000Hz$ as the controller sampling time indicating noise free input as well.

The same input data as used for identification in Section 6.3.1 was used for simulation. A PI- controller was set up in Simulink using the same parameters as estimated for the true system. The simulations were set up to make it hard to estimate the PI- controller. This was done by varying the initial conditions of the PI- controller through the simulations. Various noise realisations was added to the known control input in the simulations. This noise was added with purpose to increase the difficulty to estimate the PI- parameters accurately. There are no indications on noise in the real system but if the parameters can be estimated with noise present then they should definitely do that without noise. Simulations was performed both in noise free setup and also low-pass filtered and band-pass filtered white noise. Figure 7.1 shows the frequency representation of the input signal for estimation data together with its corresponding noisy version used in simulation.

Figure 7.2 and 7.3 shows prediction accuracy for dynamometer excited ramp data and engine excited validation data based on the simulations. First of, one can see that in the noise free case the simulated output is very accurate which indicates that there should be no problems estimating parameters and initial condition using ramp data. Even when noise is present a good prediction is obtained keeping the frequency content on the input disturbances in mind. Table 7.1 shows that indeed the parameters are estimated accurately even if the low frequency noise causes a minor error. The conclusion from the simulations must be that if SC had been a pure PI- controller it would not have failed predicting the dynamometer excited

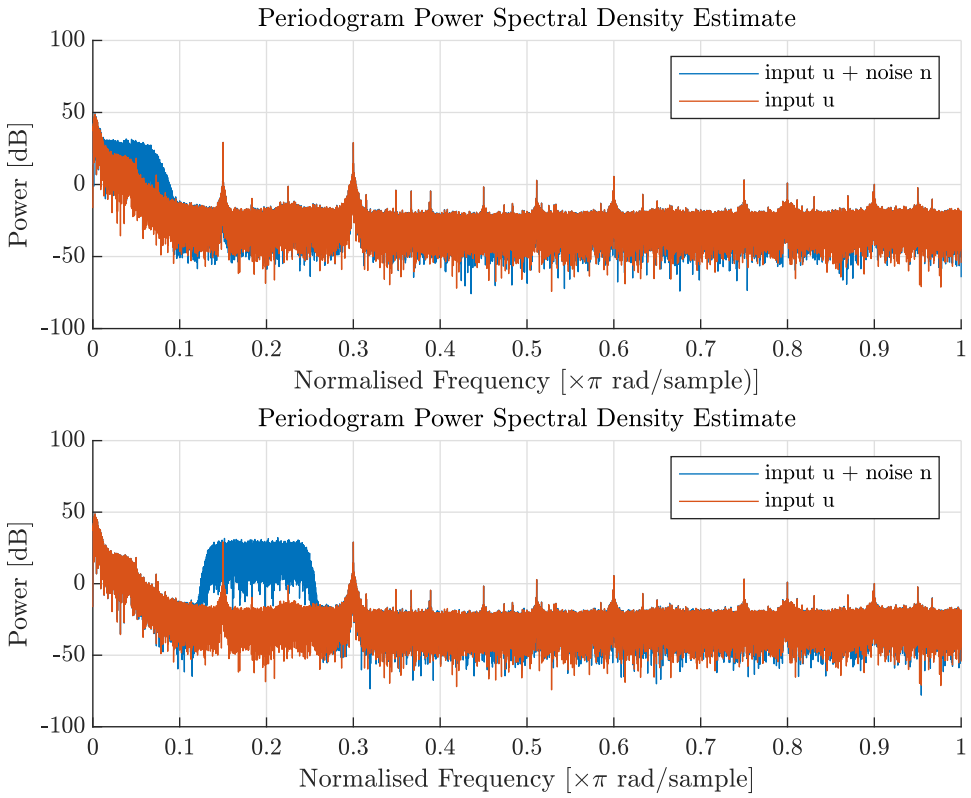

Figure 7.1: Periodogram showing the frequency content of the input for simulation. The red represents the known input used for identification. Blue corresponds to the actual input used in simulation with added noise. The SNR is 13 for low-pass noise and 8 for the band-pass noise.

ramp data as shown in Section 6.3.1. Thus there must be something more than just a PI- controller that is active when there is changes in dynamometer speed reference.

Table 7.1: Parameter estimates of the PI- parameters for the various simulations. Simulation parameters are the parameter that was used in simulation to obtain output data for identification. The other parameters are the estimated ones using various noise in simulation.

	k_p	k_i
Simulation parameter	0.9385	1.8650
Noise free parameter estimate	0.9385	1.8650
Low-pass noise estimate	0.9388	1.8896
Band-pass noise estimate	0.9385	1.8650

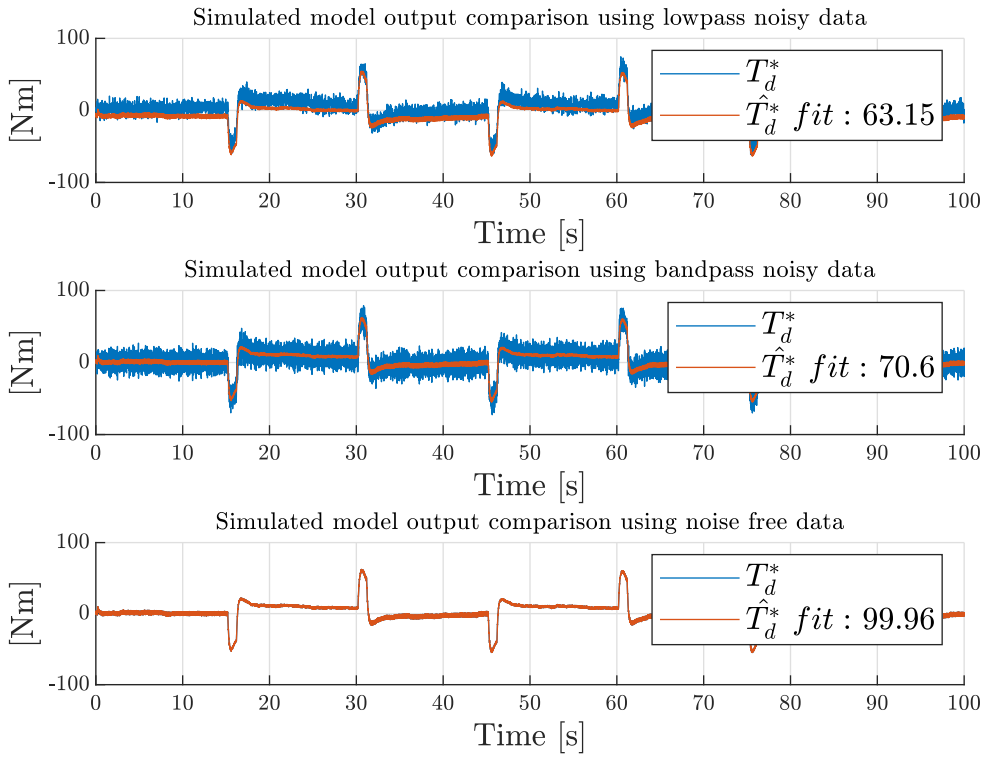

Figure 7.2: Model output comparison of data obtained through simulation of PI-controller as SC. In this case the dynamometer excited ramp speed data was used. At the top are the results using low frequency noise and in the middle band limited noise. At the bottom is the noise free case. It can be seen that the model output is a good fit for all cases. It cannot be expected to follow the noisy output perfectly since the noisy input is unknown. For the low frequency noise this mismatch also appears as an offset between simulated and true output. In this figure the simulated output lies below the true output but this varies slowly with time.

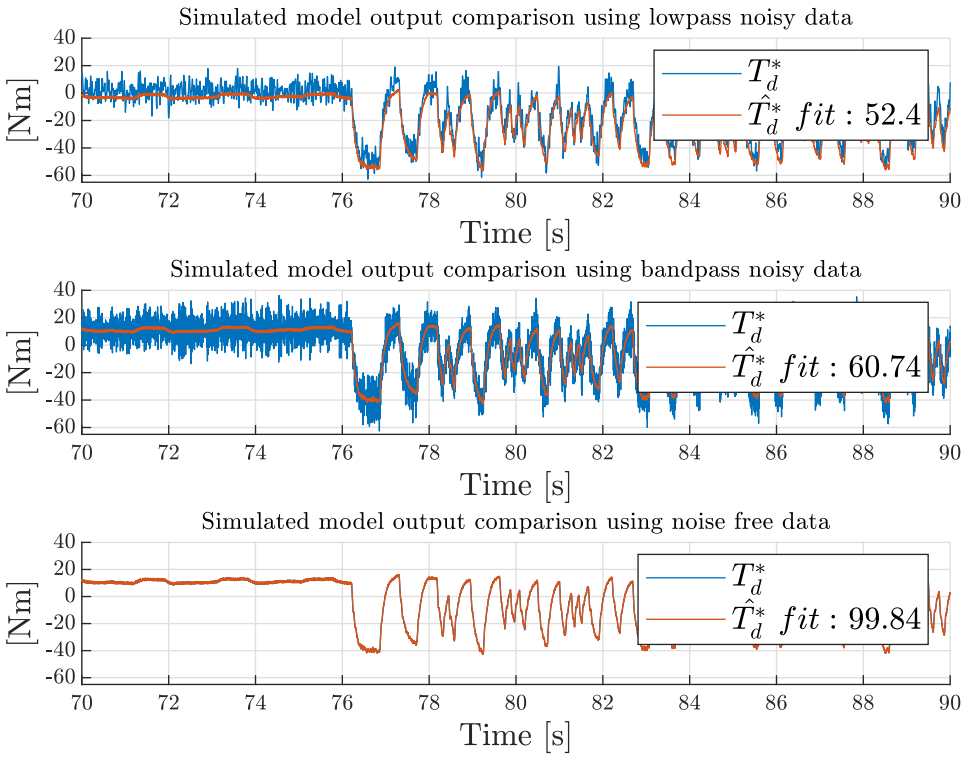

Figure 7.3: Model output comparison of data obtained through simulation of PI-controller as SC. In this case the engine excited binary sequence data was used. At the top are the results using low frequency noise and in the middle band limited noise. At the bottom is the noise free case. The results are similar compared to what can be seen in ramp data case in Figure 7.2 for the different types of noises.

7.2 Bode Model Study

In this part some post identification analysis of the complete model structure introduced in Section 6.2 and shown in Figure 6.4 (The model of FOC has been removed based on the discussion in Section 6.3.2) is performed. More specifically the submodels that was obtained through the parameter identification is combined to calculate the loop transfer from the input signals to suitable output signal. This is done both for dynamometer speed control mode NT and dynamometer torque control TN. The latter is obtained by breaking up the speed feed back loop and treating the airgap torque T_d as a pure input. As stated in Section 6.3.4 the value of the engine inertia J_e is subject to some uncertainties. This must be kept in mind throughout this chapter. Even though the results vary to some extent when trying different values of J_e the general behaviour is the same.

Since the PI- controller in SC has a transmission delay it is technically a non minimum phase. Such systems are commonly modelled using the Padé approximation [11]. The time delay here is very small (1 ms) however and has instead been neglected. Figure 7.4 shows the bode plot of the loop transfer from the two inputs in dynamometer speed control mode with dynamometer speed chosen as output. It can be seen that for low frequencies the gain from speed reference to speed equals one while the torque of the engine is dampened significantly. This is expected since the dynamometer should be able to control the speed following low frequencies. It can also be seen that a certain frequency band the engine is less damped and thus are able to affect the dynamometer speed. A resonance peak can also be seen to the right. This peak is even more prominent in Figure 7.5 which shows the loop transfer from both dynamometer and engine torque (T_d & T_e) to the shaft torque $T_{d,shaft}$. The gain is inversely proportional to the inertia which is why the gain is larger on T_e.

The peak in the gain of Figure 7.5 is located at $18Hz \approx 113rad/s$. In terms of combustion frequency this corresponds to a engine speed of 539 rpm. This is not surprising since self oscillations has been observed in the test beds for very low speeds. To further connect the model to reality the sine input test was used. In this test the dynamometer is controlling T_d with sine waves as input while the engine is aiming at constant speed. The content at the specific sine wave frequency is much larger in the input signal T_d compared to the engine input. By applying a band-pass filter around the sine wave frequencies to the output $T_{d,shaft}$ a sine wave mainly coming from the input T_d was obtained. The amplitude could then be calculated as

$$A = \sqrt{2}T_{d,shaft}^{RMS} \tag{7.1}$$

providing the gain at the specific frequency. This was done for all sines and the results are plotted against the model in Figure 7.6. The result is that the model seems to fit the experiments quite well giving some confidence to it. The model is given as

$$\frac{T_{d,shaft}}{T_d} = \frac{H_d H_{shaft}}{1 + H_{shaft}(H_d + H_e)} \tag{7.2}$$

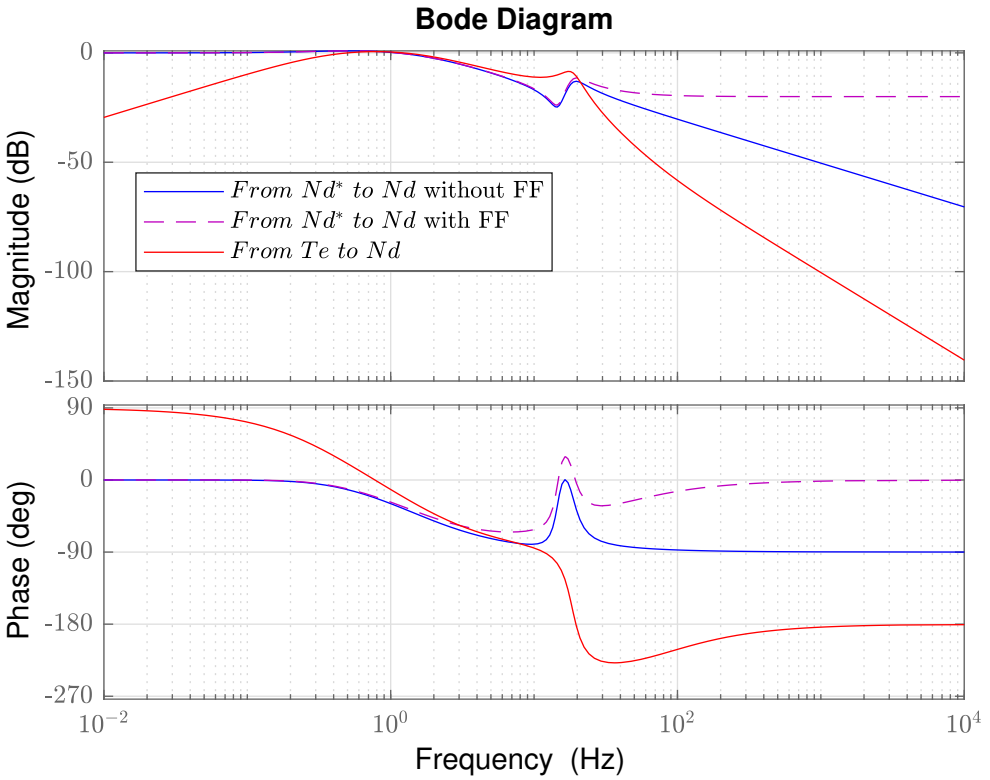

Figure 7.4: Bode plot for the loop transfer from the two inputs of the complete system model in speed control. In blue the transfer function from dynamometer speed reference to dynamometer speed is represented disregarding the feed forward. In magenta the same is shown including the feed forward. In red the transfer function from engine torque to dynamometer speed is shown.

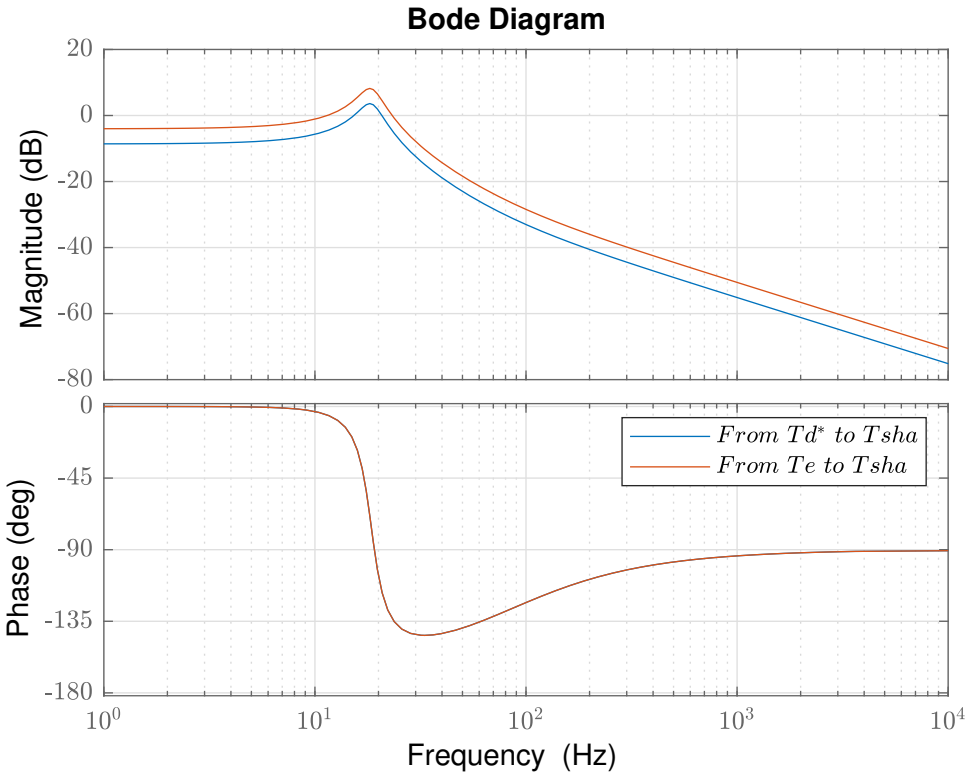

Figure 7.5: Bode plot for the loop transfer from the two inputs of the complete system model in torque control. The output in this case is the shaft torque $T_{d,shaft}$. In blue the transfer function from dynamometer airgap torque T_d to this output is represented. In red is the same from engine torque T_e.

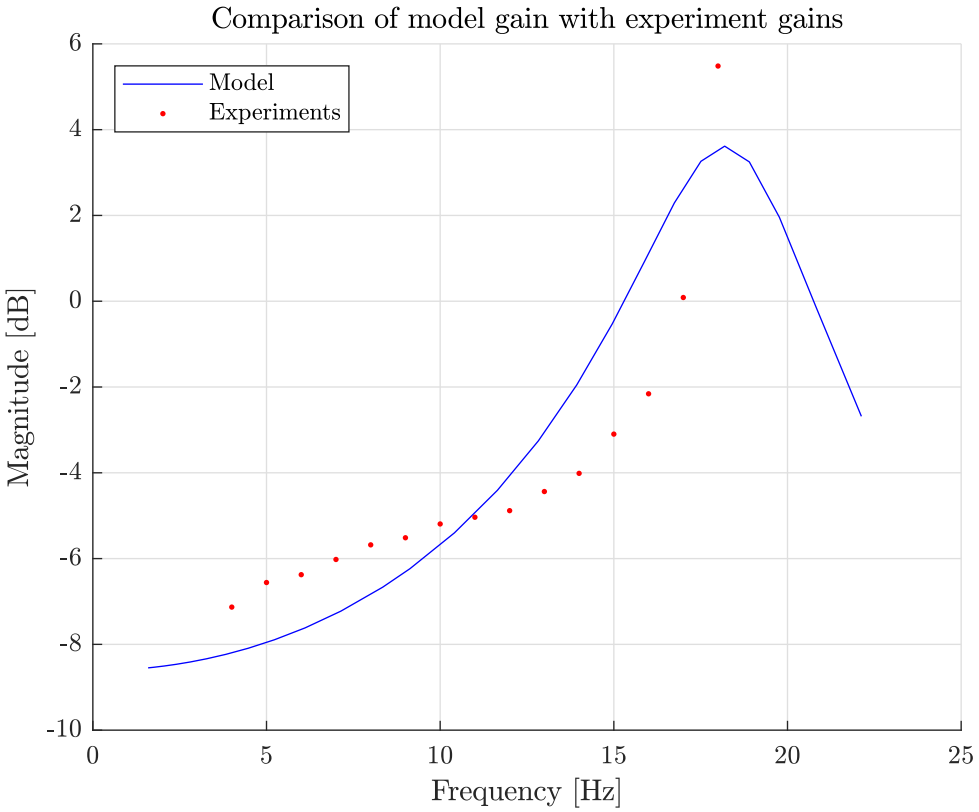

Figure 7.6: This plot shows a comparison of the bode gain plot of the model in torque control with data from experiments. Experiments where sine waves of various frequencies were used as the input T_d was performed. The estimated gain from these experiments are plottet in red at corresponding frequency. The model gain is plotted in blue.

giving away the parameters affecting the plot shown in Figure 7.6.

7.3 Simulate Complete Model Using Test Data

In this section the results from simulating the complete model in Simulink is shown. Just as before this simulation relies on the accuracy of the parameter value J_e taken from the automation system. Simulations using data measured from actual experiments was used. Simulations for both control modes TN and NT was performed using T_e together with N_d^* or T_d as model input. The fact that T_e is not available had to be addressed by calculating it from N_e and $T_{d,shaft}$. This gives an approximation of what T_e was during the experiment. This relies on the accuracy of numerical differentiation of N_e and the validity of the model assumption that $|T_{d,shaft}| = |T_{e,shaft}|$.

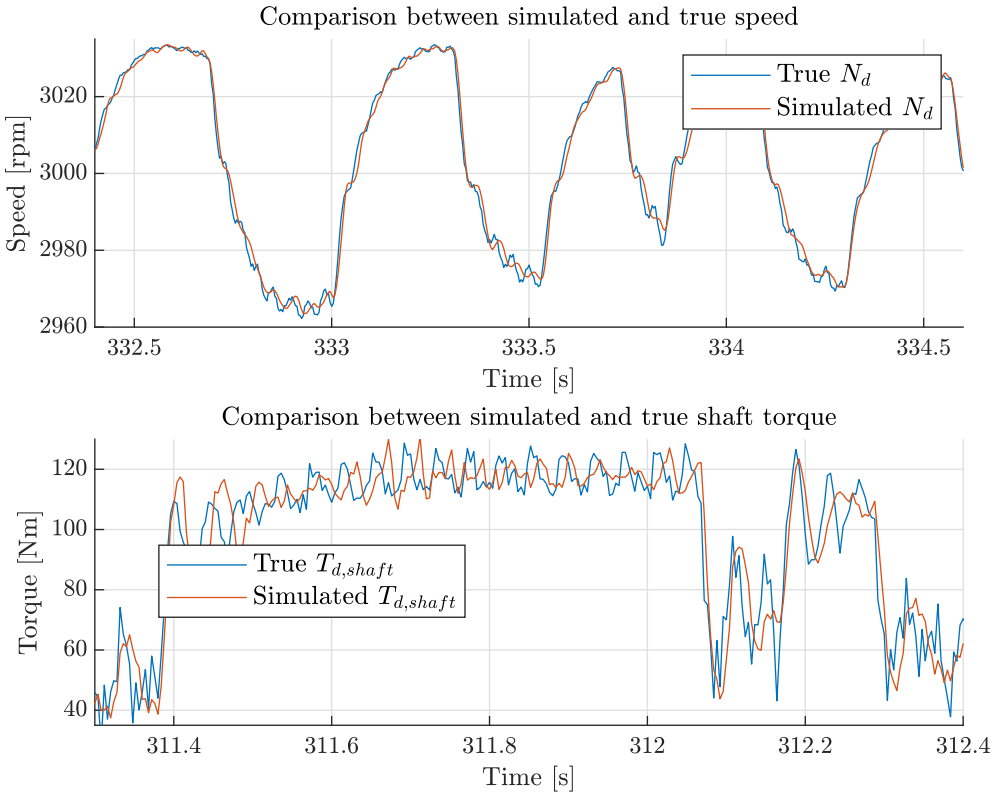

Figure 7.7: Simulation of the binary sequence experiment (see Section 4.2) where the dynamometer is controlling the speed.

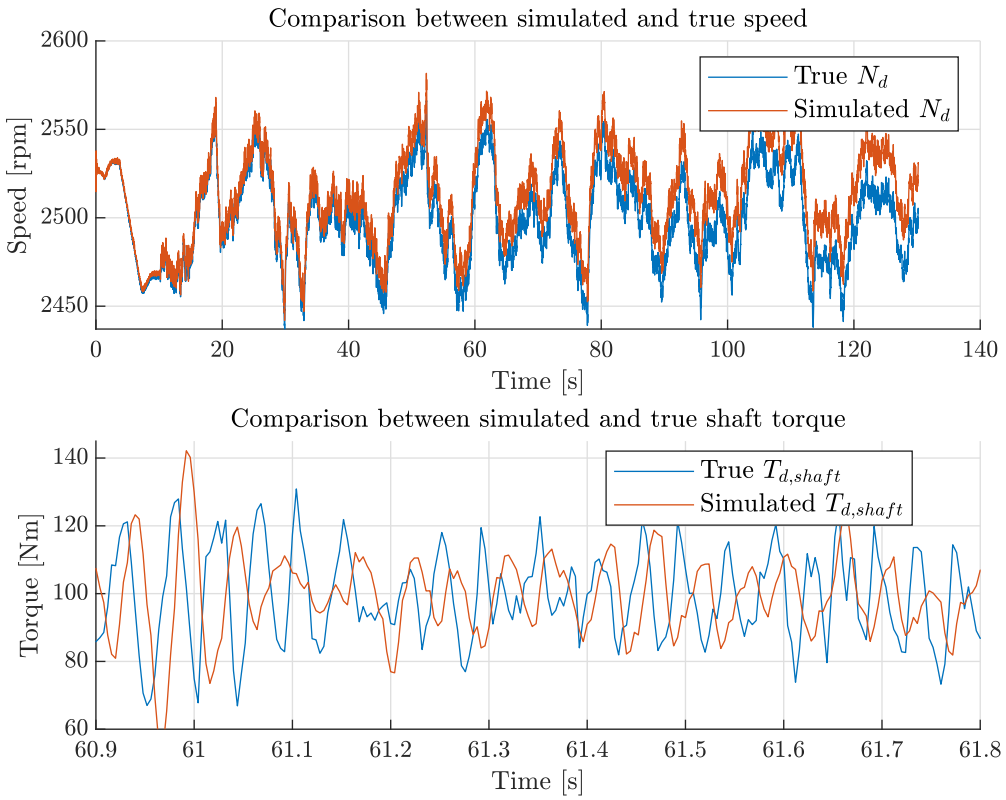

Figure 7.8: Simulation of the dynamometer white noise excitation (see 4.3).

8

Discussion and Future Work

This thesis has evaluated a method on development of a simulation model of a dynamometer including control system and shaft. An analysis on how the DTB test cell is set up has been performed. Experiments aiming at providing data for system identification has been designed and performed. A simple simulation model has been developed using system identification. Based on the results obtained from that process the properties of the various system signals has been analysed. Also the valuable experiments has been sorted out and new experiments that may provide data more suitable for some identification has been proposed.

This project aimed to consider the dynamometer including control system and shaft. These were modelled end estimated separately in this project where there were essentially three important submodels. These were the speed controller SC, the electric part of the dynamometer including torque control FOC and the shaft model. It was shown that the speed controller seems to consist of a feed back PI- controller and some sort of feed forward. Some correlation between absolute dynamometer speed and feed forward could be seen possibly indicating friction compensation. Also some acceleration dependency of N_d^* could be seen. As for future work this project proposes a new experiment where the excitation in dynamometer reference is more complex enabling the identification of the feed forward more confidence. It might be beneficial to perform this experiment once when the engine is controlling torque and once controlling throttle α. This could expose if the feed forward is dependent on what the automation system is controlling at the engine. The next important submodel is the FOC. From the data in this project nothing more could be said about the FOC than the fact that it suppresses large frequencies. If one would like to model the FOC in detail one would have to reconfigure the automation system to sample T_d^* and T_d in a higher rate. Measurements are available in the system at a rate of about 4 kHz but logged in a slower rate. The authors of this thesis does not consider a more accurate model of the FOC a matter of priority however. Instead focus should be placed on identification of the feed forward and the last important submodel that is the shaft. The shaft turned out to be the most difficult submodel to estimate. Other projects has addressed this task with some success. Unfortunately the experiment data that was gathered in this project lacks the type of excitation needed. Therefore a more simple method was proposed in this project. It described the dynamics to some extent as was seen in Chapter 7 but a more precise model is necessary in order for the simulation model to be useful. Therefore it is proposed as a matter of priority to run new experiments using less excitation on the engine as stated in Section 4.6.

Bibliography

[1] B. Drury, *The control techniques drives and controls: Handbook, emerson*, 2009.

[2] A. M. Trzynadlowski, *The field orientation principle in control of induction motors*. Springer Science & Business Media, 2013.

[3] T. Glad and L. Ljung, "Modellbygge och simulering", *Linköping University. Second edition. Studentlitteratur*, 2004.

[4] L. Ljung, Ed., *System Identification (2Nd Ed.): Theory for the User*. Upper Saddle River, NJ, USA: Prentice Hall PTR, 1999, ISBN: 0-13-656695-2.

[5] L. LJUNG, "System identification toolbox for use with matlab user's guide", 1 vol. (pagination multiple) : ill., 24 cm, 1995, Includes index.

[6] G. James, D. Witten, T. Hastie, and R. Tibshirani, *An introduction to statistical learning*. Springer, 2013, vol. 112.

[7] M. Ahsanullah, B. G. Kibria, and M. Shakil, *Normal and student's t distributions and their applications*. Springer, 2014, vol. 4.

[8] A. H. Feiveson, *Explanation of the delta method*, `https://www.stata.com/support/faqs/statistics/delta-method/`, [Online; accessed 16-July-2018],

[9] G. J. McLachlan, "Mahalanobis distance", *Resonance*, vol. 4, no. 6, pp. 20–26, 1999.

[10] R. Eisele, *How to plot a covariance error ellipse*, `https://www.xarg.org/2018/04/how-to-plot-a-covariance-error-ellipse/`, [Online; accessed 11-August-2018], 2018.

[11] B. Lennartson, *Reglerteknikens grunder*. Studentlitteratur, 2000, vol. 2002.

[12] M. Tallfors, "Parameter estimation and model based control design of drive train systems", PhD thesis, KTH, 2005.

[13] P. Langthaler and L. del Re, "Identification of driveline parameters using an augmented nonlinear model", in *16th IFAC World Congress*, 2005.

[14] L. Ljung, *System identification toolbox: user's guide*. Citeseer, 1995.

[15] MathWorks, *delayest*, `https://se.mathworks.com/help/ident/ref/delayest.html`, [Online; accessed 2-August-2018],